Figure 3. Identification of FV-infected cells in the thymus. Mice were infected with 1,000 SFFU of FV. (A) At day 14 post infection, cells in the thymus were isolated and stained with the indicated Abs. Shown are frequencies of F-MuLV gp70$^+$ cells among indicated populations as described in Figure 2. Differences in means between uninfected and FV-infected groups were analyzed by two-way ANOVA with Bonferroni's corrections for multiple comparisons: *, $p<0.0001$; †, $p<0.001$; ‡, $p<0.05$. (B) Shown are representative staining patterns for cell surface gp70 and p15^{gag} of each thymocyte population. (C) Representative frozen sections of the thymus from FV-infected mice (14 days post infection) were stained for CD11c and F-MuLV gag p30 (top), cTEC-specific ER-TR4 and F-MuLV gag p30 (middle), or mTEC-specific ER-TR5 and F-MuLV gag p30 (bottom). Arrowheads indicate cells double positive for the indicated cell surface marker and the viral antigen. A larger view field of the sections shown here can be seen in Figure S3. (D) Mice were infected with 1,000 SFFU of FV. At day 14 after infection, cells in the thymus were isolated, stained with the indicated Abs, and FACS sorted into the indicated populations as described in Figure 2. Cells were cocultured with *M. dunni* cells to enumerate F-MuLV infectious centers. Each symbol represents cells from an individual mouse. Dashed lines indicate the detectable limits (e.g. maximum available numbers of DCs and TECs used in this experiment were 1×10^5). Data are representative of two independent experiments with essentially equivalent results.
doi:10.1371/journal.ppat.1003937.g003

in age-matched uninfected mice (Figure 4B, C). These results so far revealed that the basic function of the thymus appeared to be retained in FV-infected mice.

However, since viral antigen expression was found in the thymic DCs and TECs (Figure 2 and 3), we speculated that processed viral antigens could be presented in the context of MHC class I and class II molecules on the surfaces of these cells, which might eliminate thymocytes bearing viral antigen-reactive T-cell receptors (TCRs) via negative selection. To test this, we employed a thymus transplantation approach in which thymic lobes from either FV-infected (4–8 weeks post infection) or age-matched uninfected mice were transplanted into syngenic recipients that have been thymectomized and treated with T-cell-depleting antibodies prior to the transplantation (Figure 5A). Transplantation of thymic lobes from FV-infected or uninfected mice was equally able to reconstitute peripheral T cells as we observed similar frequencies of CD8$^+$ T cells in the blood at 6–8 weeks post transplantation (Figure 5B). Note that we have checked spleen weights and F-MuLV gp70 expression on B cells and Ter119$^+$ erythroblasts in the recipient mice that received the thymus from FV-infected donors, and found no evidence of splenomegaly or significant increase in gp70$^+$ cells (Figure S4). These results clearly indicate minimal, if any, transmission of FV via the transplantation of thymic lobes from FV-infected donors. In both recipient groups, comparable frequencies and numbers of influenza nucleoprotein (NP)-specific CD8$^+$ T cells were detected in the spleens following infection with influenza virus ×31 (Figure 5C, D), suggesting that CD8$^+$ T cells that arose from the FV-infected thymic transplant were bona fide mature T lymphocytes with the intact capability to respond to an FV-unrelated antigen. Importantly, however, following challenge with FV antigen-bearing FBL3 tumor cells, minimal evidence of FV-specific tetramer binding on CD8$^+$ T cells was observed in mice transplanted with FV-infected thymuses, while control mice transplanted with uninfected thymuses showed significantly higher levels of FV-specific CD8$^+$ T cell expansion at the peak of response (Figure 5C, D). This was indicative of an incapability of FV-infected thymus to generate FV-specific naïve CD8$^+$ T cells. Overall, the above data clearly demonstrated that thymic infection with FV resulted in the depletion of thymocytes expressing TCRs specific for FV antigens.

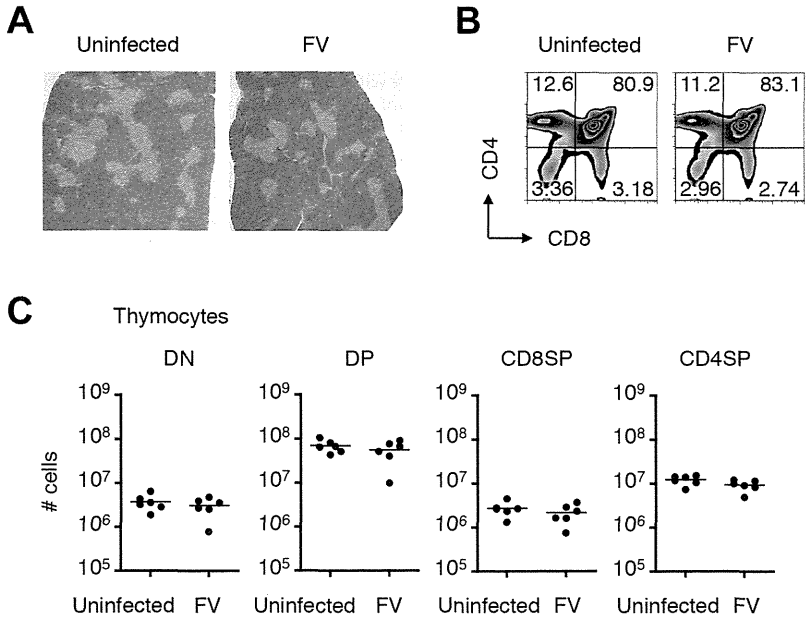

Figure 4. Infection of thymus with FV has no influence on numbers and frequencies of thymocyte populations. Mice were infected with 1,000 SFFU of FV. (A) Representative hematoxylin- and eosin-stained thymus sections from FV-infected (21 days post infection) or age-matched uninfected mice. Thymocytes isolated from the same experimental mice were stained for CD4 and CD8. Shown are representative dot plots (B) and actual numbers of each thymocyte population (C). Each symbol represents an individual mouse. No significant differences were observed between the groups. Data are representative of two independent experiments with essentially equivalent results.
doi:10.1371/journal.ppat.1003937.g004

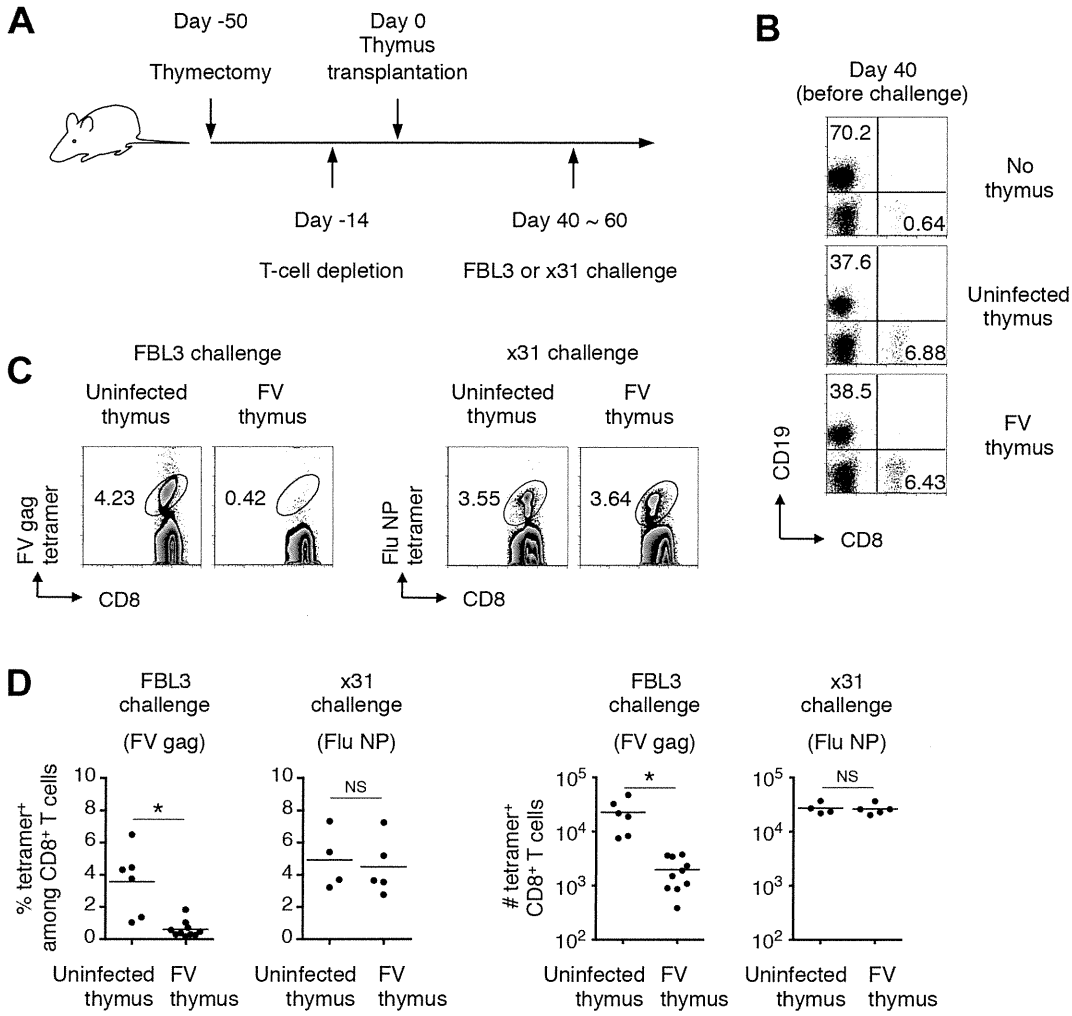

Figure 5. Infection of thymus with FV leads to clonal deletion of FV-specific thymocytes. (A) To make a T cell-free microenvironment in $B6AF_1$ mice, day 5 neonatal pups were thymectomized, and 5 weeks later were injected intraperitoneally with depleting Abs for both CD4 and CD8. Two weeks later, a thymic lobe from either FV-infected (2–3 weeks post infection) or age-matched uninfected mice was grafted under the kidney capsule. (B) At day 40 after transplantation, splenocytes were isolated and stained with the indicated Abs. Shown are representative staining patterns for CD8 and CD19. (C) Six weeks after transplantation, when peripheral CD8 T cells were reconstituted, mice were challenged with either FV-antigen bearing FBL3 tumor cells or influenza virus ×31. Splenocytes were isolated at 10–14 days post challenge, and stained with the indicated Abs and either F-MuLV gag_{75-83}/D^b or Flu $NP_{366-374}/D^b$ tetramer. Shown are representative staining patterns for CD8 and each tetramer among $CD8^+$ T cells. (D) Shown are frequencies of $tetramer^+$ cells among $CD8^+$ T cells (left panels), and actual numbers of $tetramer^+$ $CD8^+$ T cells (right panels). Averages of % and actual numbers of $tetramer^+$ cells were compared between uninfected and FV-infected groups by two-tailed Welch's *t*-test, as variances in both cases were not regarded as equal. *, $p<0.021$; NS, not significant.
doi:10.1371/journal.ppat.1003937.g005

Thymic DCs and TECs are the direct deleters of FV-specific thymocytes

Given that the dissemination of FV to the thymus led to the apparent negative selection of viral antigen-reactive thymocytes, we next wished to determine which cell populations in the FV-infected thymus were responsible for this negative selection. To do this, we performed the fetal thymus organ culture (FTOC) [22]. To utilize TCR-transgenic T cells, we first generated a recombinant F-MuLV, F-MuLV-OVA, expressing the K^b-restricted OVA-derived peptide $OVA_{257-264}$, for which the OT-1 $CD8^+$ T cells are reactive, and the activation of OT-1 $CD8^+$ T cells upon stimulation with F-MuLV-OVA-infected cells was confirmed (Figure S5). As the SFFV-induced massive proliferation of erythroid cells was required for effective dissemination of F-MuLV into the thymus (Figure S2), mice were either inoculated with FV alone (a mixture of approximately equal infectious titers of F-MuLV and SFFV) or FV plus F-MuLV-OVA (abbreviated as FV-OVA). To ensure that F-MuLV-OVA could infect SFFV-infected erythroid cells by overcoming the possible receptor interference with wild-type F-MuLV, a twice larger infectious titer of F-MuLV-OVA was given relative to the titer of F-MuLV in the FV complex used. A mixture of thymocyte-depleted thymic stromal cells from uninfected fetus (day 15 of gestation) and FACS-sorted OT-1 DP thymocytes were cultured in the presence of a third population (each single population purified from the thymus of either FV- or FV-OVA-infected mice) as a candidate deleter cell population (Figure 6A). In the absence of the third population, the development of OT-1 CD8 single positive (SP) cells was observed at day 5, which was apparently reduced when OVA-expressing E.G7 cells were added in the culture (Figure S6A). The addition of control EL-4 cells did not affect the generation of

CD8 SP cells, revealing the reliability of this approach to test the ability of the third population to induce antigen-specific negative selection. Because the numbers of OT-1 CD8 SP cells recovered from the FTOC varied significantly in each experiment, perhaps due to the technical difficulty in simultaneously preparing three different groups of cells (stromal cells, OT-1 DP thymocytes, and third populations purified from the thymus of virus-infected mice; see Figure 6A), we evaluated the influences of third populations on the development of OT-1 CD8 SP cells by calculating the relative reduction of the frequency of OT-1 CD8 SP cells in an experimental culture compared to those in the control culture (without adding the third population) in each set of experiments (Figure S6B). As shown in Figure 6B, the addition of thymocyte populations from FV-OVA-infected mice had no influence on the development of OT-1 CD8 SP cells, indicating that despite the high level of FV infection and extensive antigen expression, FV-infected thymocytes did not actively induce the negative selection of viral antigen-specific thymocytes. In contrast, we observed a significant reduction in the frequencies of OT-1 CD8 SP cells when the cultures contained either thymic DC populations (except pDC) or TEC populations from FV-OVA-infected mice (Figure 6B and Figure S6B). Although some reductions in the frequency of OT-1 CD8 SP cells were also observed when DCs and TECs from FV-infected mice were added in the culture, the extent of CD8 SP cell reduction was significantly higher when thymic DCs or mTEC from FV-OVA-infected mice were added (Figure 6B and Figure S6B). The data thus far suggest that presentation of viral antigens on the thymic DCs and TECs seems to play a key role in inducing clonal deletion of viral antigen-reactive thymocytes.

FV-specific CD8$^+$ T cells, if recruited during the chronic phase of infection, can differentiate into functional memory CD8$^+$ T cells

In the case of other models of chronic infection in which the pathogens do not disseminate to, or disappear from, the thymus [e.g. polyoma virus infection or more than 30 days after lymphocytic choriomeningitis virus (LCMV) clone 13 infection], newly recruited virus-specific CD8$^+$ T cells can be primed and differentiate into functional memory CD8$^+$ T cells [5,6]. Therefore, we hypothesized that if FV-specific CD8$^+$ T cells were generated in animals chronically infected with FV, such recent thymic emigrants (RTEs) may be able to undergo a process of post-thymic maturation, and then be primed and differentiate into antiviral CD8$^+$ T cells with a superior functional capacity as compared to the severely exhausted memory CD8$^+$ T cells in the periphery. To test this possibility, we investigated if the immune environments in chronically infected animals influence the process of post-thymic maturation in the periphery. To this end, we used *Rag1*-GFP knock-in mice as a tool to distinguish RTEs based on the expression of GFP within peripheral T cells, and first analyzed total, mostly FV-nonreactive, CD8$^+$ T cells since FV-infected mice lack the generation of FV-specific RTEs as shown above. Total numbers of GFP$^+$CD8$^+$ T cells in the spleens of FV-infected and age-matched uninfected mice were comparable at 6 weeks post infection (Figure S7A, B), confirming the unaffected T-cell generating function of the FV-infected thymus (Figure 4). Importantly, in the FV-infected mice, while a large proportion of GFP$^-$CD8$^+$ T cells showed the highly activated phenotype (CD44^{hi}CD69$^+$PD-1^{hi}), GFP$^+$CD8$^+$ RTEs at 6 weeks post infection showed minimal signs of abnormal activation as they

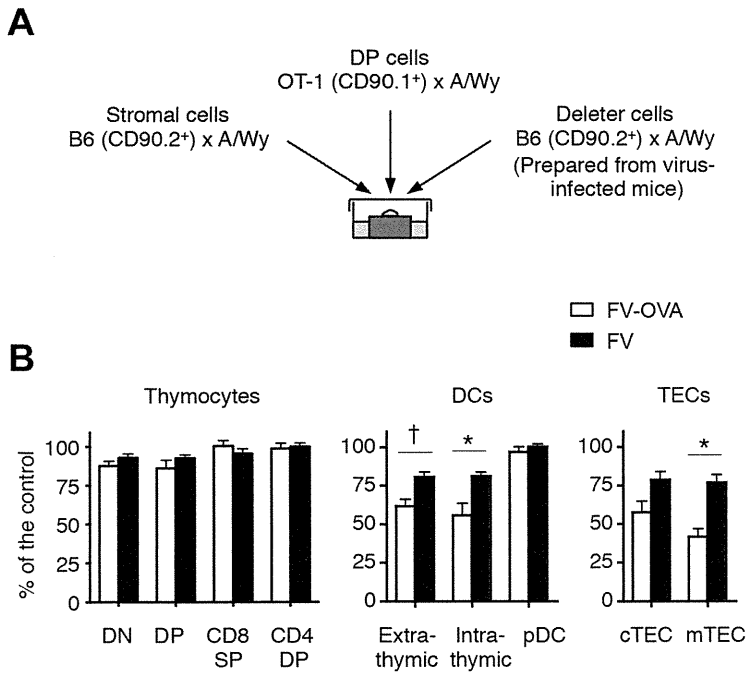

Figure 6. Thymic DCs and TECs are the major deleters of FV-specific thymocytes. (A) Thymic stromal cells of B6AF$_1$ mice were prepared from E15.5 fetal thymus lobes. OT-1 DP thymocytes were sorted from adult (OT-1-Thy1.1 × A/WySnJ)F$_1$ mice. Thymocytes, thymic DCs and TECs from FV-OVA infected mice (21 days post infection) were sorted into each population as indicated in Figure 2. Cells were mixed and cultured as a reassembled organ for 4 days. (B) Shown are relative percentages of CD8 SP cells as compared to the control. The percentage of the control value was calculated by [(% of CD8 SP cells in the experimental culture)/(% of CD8 SP cells in the control culture)] ×100 (see Figure S5). Averages were compared between FV-OVA- and FV-infected groups for each third cell population by two-way ANOVA with Bonferroni's correction for multiple comparisons, and statistically significant differentiations are indicated: *, $p<0.01$; †, $p<0.05$.
doi:10.1371/journal.ppat.1003937.g006

mostly remained $CD44^{lo}CD69^{-}PD\text{-}1^{lo}$ (Figure S7C). Since GFP expression is reduced concurrently with Rag expression ceasing 2–3 weeks after TCR rearrangements (1–2 weeks after exiting from the thymus) [23], $GFP^{+}CD8^{+}$ T cells detected at 6 weeks post infection should have been generated after FV infection, and thus the above results on unactivated phenotypes indicate that the RTEs did not receive bystander inflammatory signals even in the chronically infected environment. A transient increase in the proportion of activated ($CD44^{hi}CD69^{+}PD\text{-}1^{hi}$) $CD8^{+}$ RTEs at the peak of infection (2 weeks post FV infection) also supports this idea (Figure S7C). At 6 weeks post infection, gradual loss (CD24) and gain (CD127 and Qa2) of surface antigen expression by $CD8^{+}$ RTEs revealed a prototypic status of post-thymic maturation in FV-infected mice (Figure S6D) [23]. Furthermore, although $CD8^{+}$ RTEs typically have only a weak capacity to produce cytokines [24], $GFP^{+}CD8^{+}$ T cells in FV-infected mice were capable of producing IFN-γ and IL-2 upon stimulation with anti-CD3 antibody at levels comparable with those in the uninfected mice (Figure S7E, F). These results indicate that chronic infection with FV has little, if any, impact on the post-thymic maturation of RTEs in general.

Nevertheless, it is possible that chronic infection with FV may create an immune suppressive environment that impairs the peripheral priming of $CD8^{+}$ T cells. To examine this possibility we next asked whether naïve (post-thymically matured) $CD8^{+}$ T cells could be adequately primed in animals chronically infected with FV. To do this, mice were infected with FV, and 6–8 weeks later were further infected with an FV-unrelated pathogen, influenza ×31 (Figure 7A). Eleven days post ×31 infection, FV-infected mice nevertheless developed robust anti-influenza $CD8^{+}$ T cell responses detectable with MHC tetramer staining and antigen-specific IFN-γ production in association with the surface expression of CD107a (Figure 7). Importantly, levels of the influenza NP-specific $CD8^{+}$ T cell responses in the FV-infected mice were as high as those in the uninfected mice, indicating that chronic FV infection had minimal impact on the induction of influenza-specific $CD8^{+}$ T cell responses (Figure 7). Differentiation of functionally competent memory $CD8^{+}$ T cells was also observed in FV-infected mice at a later stage of influenza virus infection (data not shown). Similar to the model shown in Figure S1, however, FV-specific $CD8^{+}$ T cells generated in the same FV-infected animals were severely exhausted at any time-point examined in this experimental setting (data not shown). These results indicate that even in the situation where the functions of FV-specific $CD8^{+}$ T cells were severely compromised (Figure S1), animals chronically infected with FV had no, if any, defects in mounting FV-unrelated $CD8^{+}$ T cell responses.

Based on the above observations that FV-unrelated $CD8^{+}$ T cells can be activated in a chronically FV-infected environment, we next investigated whether FV-specific naïve $CD8^{+}$ T cells recruited from FV-uninfected exogenous sources can be primed and differentiate into functional memory $CD8^{+}$ T cells in the recipients during the chronic phase of infection. To do this, naïve ($CD44^{lo}$) OT-1 cells were transferred into mice that had been infected chronically with either FV or FV-OVA (Figure 8A). As shown in Figure 8B, a small but significant proportion of transferred OT-1 cells were found to be primed in the presence of persistent OVA antigen expressed from FV-OVA at 4 weeks post transfer. As expected, the expression of PD-1 on the newly primed OT-1 cells was significantly lower than that on highly exhausted endogenous OVA-specific $CD8^{+}$ T cells (Figure 8C, D), indicating that newly primed virus-specific $CD8^{+}$ T cells were not exhausted. Interestingly, transferred OT-1 cells were rarely recruited to the BM (Figure 8C), a hot spot of persistent antigen presentation (Figure S1B). This might explain why newly primed OT-1 cells were not instantly exhausted. Slightly lower levels in the expression of the recent activation marker CD69 on OT-1 cells as compared to that on endogenous OVA-specific $CD8^{+}$ T cells is probably due to the priming of naïve OT-1 cells needing professional APCs while endogenous, antigen-experienced OVA-specific $CD8^{+}$ T cells can be reactivated by most virus-infected cells (Figure 8C, D). Intracellular cytokine staining of antigen-experienced ($CD44^{hi}$) OT-1 cells revealed a high-level production of IFN-γ in response to $OVA_{257-264}$ peptide stimulation, which was observed exclusively in newly primed OT-1 cells transferred in the chronic phase of infection, but not in OT-1 cells transferred prior to FV-OVA infection (thus, those primed in the early phase of infection) (Figure 8A, E, F). Moreover, newly primed OT-1 cells still retained the ability to produce IL-2, a function that disappeared primarily in the exhausted $CD8^{+}$ T cells (Figure 8E, F) [25]. OT-1 cell transfer into FV-OVA-infected mice resulted in a slight reduction in spleen weights and a significant decrease in the numbers of infectious centers (Figure 8G), indicating that late-primed OT-1 cells can control chronic infection at least to some extent. Although we cannot predict from the above observation that newly recruited FV-specific $CD8^{+}$ RTEs would control chronic infection, as the number of transferred OT-1 cells (1×10^{7}) might be non-physiological, the above results clearly demonstrate that, despite the replication-competent component of the FV-OVA in the present experiment being a mixture of F-MuLV-OVA and wild-type F-MuLV, a significant proportion of infected erythroid cells expressed the OVA epitope. These results thus provide conclusive evidence that if FV-specific naïve $CD8^{+}$ T cells are continuously recruited from the thymus even during the chronic phase of FV infection, cells newly primed with the persistent antigen can at least differentiate into the functional memory $CD8^{+}$ T cells and may contribute to FV control. Overall, the above data indicate that FV-induced central tolerance inhibits the generation of virus-specific naïve $CD8^{+}$ T cells that can otherwise be primed with FV antigens even in the chronic phase of infection, and the resultant lack of FV-reactive RTEs contributes to the observed lack of functional memory $CD8^{+}$ T cells along with the exhaustion of antigen-experienced $CD8^{+}$ T cells.

Discussion

Recognition of self-antigens in the thymus is essential for the deletion of self-reactive thymocytes. In addition, silencing selection-escaped $CD8^{+}$ T cells via abundant antigens and PD-1-mediated costimulation in the periphery is one of the mechanisms of peripheral tolerance, in addition to the suppression of self-reactive effector T cells by Tregs [26]. The data presented in our current and previous studies have demonstrated cunning strategies of murine retrovirus to evade anti-viral $CD8^{+}$ T cell immunity by modulating both central and peripheral tolerance. During the acute phase of infection, massively expanded virus-infected $PD\text{-}L1^{hi}$ erythroblasts disrupt the function of virus-specific effector $CD8^{+}$ T cells in the periphery [21]. Then, the virus disseminates to the thymus and induces viral antigen presentation by DCs and TECs just as if self-antigens are present. In fact, endogenous retroviral antigens potentially cross-reactive to the exogenous retroviruses are known to be present in the thymus and shape T cell responses to the exogenous retroviruses by inducing the negative selection of low-avidity virus-reactive T cells [27]. On the other hand, the presentation of exogenously infecting viral antigens in the thymus inhibits subsequent production of virus-specific naïve $CD8^{+}$ T cells as a source of functional memory

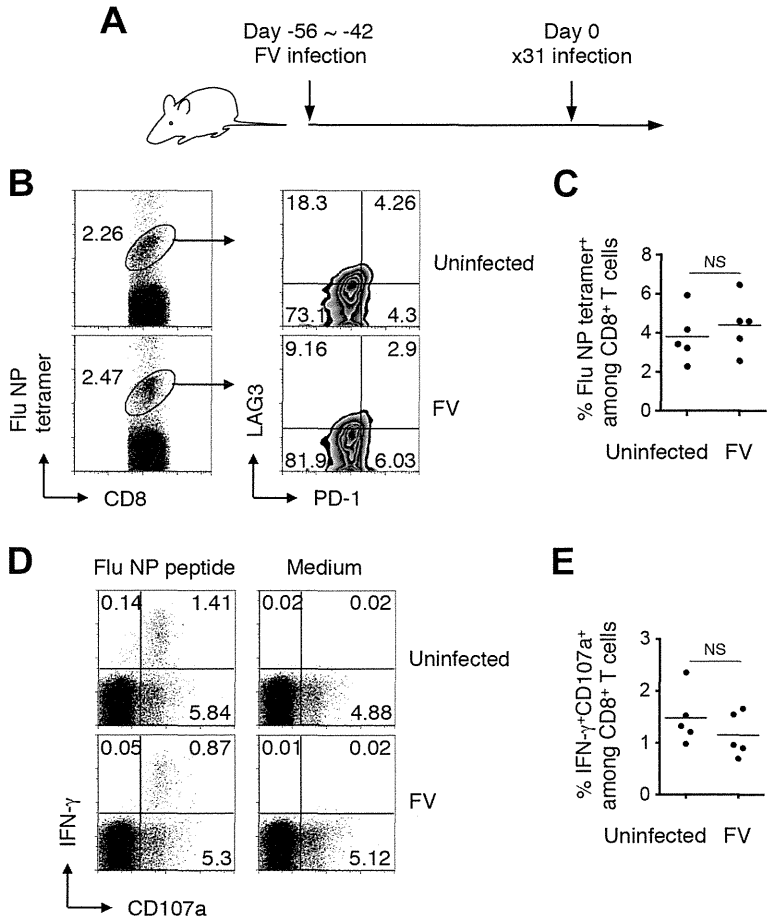

Figure 7. Generation of CD8$^+$ T cell responses in mice chronically infected with FV. (A) FV-infected (6–8 weeks post infection) and age-matched uninfected mice were challenged i.n. with influenza virus ×31. (B, C) At day 11 after ×31 infection, splenocytes were isolated and stained with the indicated Abs and Flu $NP_{366–374}/D^b$ tetramer. (B) Shown are representative staining patterns for CD8 and the tetramer of CD8$^+$ T cells, and LAG3 and PD-1 expression on tetramer$^+$ cells. (C) Frequencies of $NP_{366–374}/D^b$ tetramer$^+$ cells among CD8$^+$ T cells in the spleen. (D, E) Fractions of cells were stimulated with either $NP_{366–374}$ peptide or anti-CD3 Ab. The intracellular expression of IFN-γ and the surface expression of CD107a were measured by flow cytometry. (D) Shown are representative staining patterns for IFN-γ and CD107a of CD8$^+$ T cells. (E) Frequencies of IFN-γ$^+$CD107a$^+$ cells among CD8$^+$ T cells. Each symbol represents an individual mouse. Functionally competent influenza virus-specific CD8$^+$ T cells were detected even at day 30 post challenge (data not shown). Average percentages of tetramer$^+$ cells are not significantly different between the groups.
doi:10.1371/journal.ppat.1003937.g007

CD8$^+$ T cells in chronically infected animals as we have shown here for FV infection. Consequently, almost all virus-specific CD8$^+$ T cells in FV-infected animals lack their effector functions. Although viral replication is controlled at low levels by the production of virus-neutralizing antibodies [8], mice chronically infected with FV are highly susceptible to challenge with FV-induced tumor cells against which CD8$^+$ T cell response is required for effective elimination.

Induction of pathogen-specific central tolerance through thymic dissemination is not a unique feature of FV infection. It has been reported that neonatal infection with Gross murine leukemia virus (G-MuLV) or Moloney murine leukemia virus (Mo-MuLV) results in intrathymic viral replication that induces life-long immune nonresponsiveness to viral antigens [28,29]. It should be noted, however, that when inoculated into adult mice, Mo-MuLV is rapidly eliminated and does not cause leukemia [30]. Interestingly, experiments on intrathymic (i.t.) inoculation revealed that G-MuLV infects predominantly thymic epithelial cells, while Mo-MuLV, which does not induce tolerance following i.t. inoculation in adult mice, favors mature T cells as targets of infection in the thymus [28,31,32]. In the case of adult infection, as mentioned above, LCMV clone 13 is known to disseminate to the thymus and induce virus-specific central tolerance [33–35]. Recently, some species of *Mycobacteria* have also been reported to induce bacteria-specific T cell tolerance via thymic dissemination [36,37]. Since some extent of functional pathogen-specific CD8$^+$ T cells remain in these chronically infected animals, loss of pathogen-specific RTEs does not make a significant impact on ongoing infections [38]. Contrarily, FV infection leads to almost complete loss of functional virus-specific CD8$^+$ T cells in the periphery [21]. Furthermore, because functional antigen-specific CD8$^+$ T cells in the periphery re-enter the thymus and can delete infected APCs to abrogate central tolerance [33,34,39], early and overall exhaustion of functional FV-specific CD8$^+$ T cells in the periphery may extend viral persistency in the thymus due to ineffective viral clearance in this organ.

A question that remains is how FV initially disseminates to the thymus. The finding that CD44^{hi} DN thymocytes lack the expression of viral proteins indicates that BM-originated common lymphoid progenitor cells are unlikely to be an active transporter of the virus to the thymus. In the steady state, it has been demonstrated that conventional DCs, as well as plasmacytoid DCs

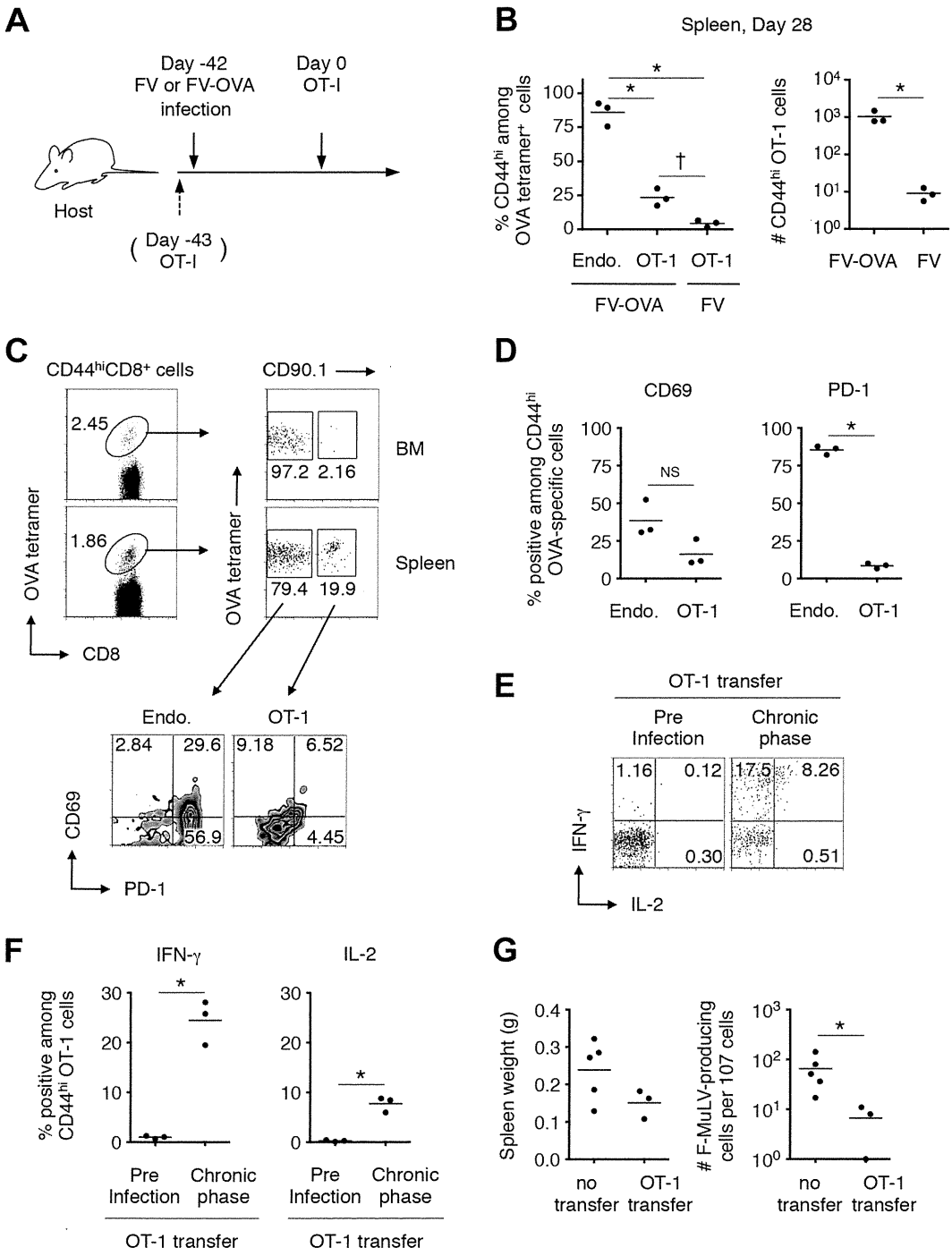

Figure 8. FV-specific CD8$^+$ T cells can differentiate into functional memory CD8$^+$ T cells if recruited during the chronic phase of infection. (A–D) B6AF$_1$ mice were infected with either FV or FV-OVA. Six weeks later, FACS-sorted naïve (CD44^{lo}) CD8$^+$ T cells (1–2×10^7) from (OT-1-Thy1.1× A/WySnJ)F$_1$ mice were transferred i.v. Splenocytes and BM cells were isolated at 28 days post transfer and stained with the indicated Abs and OVA$_{257–264}$/K^b tetramer. (B) Percentages of CD44^{hi} cells among OT-1 cells or endogenous OVA-specific CD8$^+$ T cells, and actual numbers of CD44^{hi} OT-1 cells recovered from FV-OVA- or FV-infected mice. Averages between groups in the left panel were compared by one-way ANOVA with Tukey's multiple comparison test: *, $p<0.001$; †, $p<0.05$. Averages between FV-OVA and FV groups were compared by Welch's *t*-test: *, $p=0.047$. (C) Representative staining patterns for PD-1 and CD69 among OT-1 cells or endogenous OVA-specific CD8$^+$ T cells in the BM and spleen. (D) Expression of CD69 and PD-1 on CD44^{hi} OVA-specific CD8$^+$ T cells in the spleen. Averages were compared for the two parameters between the endogenous and OT-1 cells: *, $p<0.00001<\alpha_2\,(0.05)=0.0253$ by student's *t* test with Bonferroni's correction for multiple comparisons. (E–F) A group of mice received 5×10^3 OT-1 cells 1 day prior to FV-OVA infection as a control for CD8$^+$ T cell responses that were primed by initial infection. Splenocytes were stimulated in vitro with OVA$_{257–264}$/K^b peptide. Shown are intracellular expression levels of IFN-γ and IL-2 of CD44^{hi} OT-1 cells primed at the initial infection or during the chronic phase of infection. Averages were compared for the two parameters between the preinfection transfer and chronic phase groups: *, $p=0.012<\alpha_2\,(0.05)=0.0253$ for IFN-γ and $p=0.013<\alpha_2\,(0.05)=0.0253$ by Welch's *t*-test with Bonferroni's correction. (G) B6AF$_1$ mice were infected with 5,000 focus-forming units of F-MuLV-OVA plus 2,000 SFFU of FV and naïve OT-1 cells (1×10^7) were transferred 28 days after infection. Four weeks after transfer of naïve OT-1 cells, spleen weights were measured, and splenocytes were cocultured with *M. dunni* cells to

enumerate F-MuLV infectious centers. Each symbol represents an individual mouse. *, significantly smaller in the numbers of infectious centers in comparison with those in non-transferred mice; $p = 0.0357$ by Mann-Whitney test for non-Gaussian distributions.
doi:10.1371/journal.ppat.1003937.g008

in the blood, transport peripheral self-antigens to the thymus and initiate central tolerance [40,41]. In pathological conditions, however, the activation/maturation process strongly inhibits the migration of peripheral DC populations to the thymus by modulating their chemokine receptor expression [40,41], thus preventing the unfavorable induction of acquired tolerance to the invading pathogens. However, it has become evident that in some cases, such as infections with *Mycobacteria* and highly pathogenic influenza virus, pathogen-infected DCs of an extrathymic origin can transport the infectious microorganisms to the thymus, resulting in thymic dissemination and subsequent thymic dysfunctions [36,42]. Although we do not exclude the possibility that this could be the case in FV infection, as gp70 expression was observed on extrathymic DCs in the thymus, we could not detect the production of infectious virions from any thymic DC population even at the peak of infection. Alternatively, because prior exposure to antigen enhances the migration of mature T cells to the thymus, activated T cells that are infected with the virus in the periphery, if there are any, might be another potential source in transporting the virus into the thymus. However, faint expression of gp70 on $CD44^{hi}$, CD4 SP and CD8 SP populations in FV-infected thymus makes this unlikely. Since F-MuLV can infect and replicate in endothelial cells at high levels, and the virus particles can be found in a subendothelial location of blood vessels [43,44], it is reasonable to postulate that FV disseminates to the thymus through the replication in the endothelial cells and subsequent production of viral particles to the parenchymal side, rather than via the migration of virus-infected hematopoietic cells into the organ.

Another issue to be considered is whether thymic infection with FV results in the generation of Tregs. It has become clear that thymocytes that display TCRs with higher affinity (but much lower than that induces negative selection) for thymic MHC/self-peptide ligands can develop into Tregs [45,46]. Thus, not only the induction of negative selection, but the generation of naturally occurring Tregs (nTregs) harboring TCRs reactive with non-self antigen could also be induced by thymic infection with pathogens [47]. As an increase in the number of Tregs in lymphoid organs has long been recognized in FV-infected animals [16–18,48], dissemination of the virus into the thymus might be one of the factors that cause the increase of Tregs. In fact, the observed expansion of Tregs peaked around 2 weeks post FV infection [16], approximately the same time-point that viral antigen expression in the thymus was peaking. In the recent study, moreover, adoptive transfer of $FoxP3^-$ $CD4^+$ T cells and tracking neuropilin-1 expression as a marker of nTregs revealed that Tregs that expanded after FV infection originated from thymus-derived nTregs but not from $FoxP3^-$ conventional $CD4^+$ T cells in the periphery [48]. Importantly, however, it was suggested that Tregs that expanded after FV infection lack the expression of TCRs specific for FV antigen [48,49]. Therefore, viral antigen expression in the thymus may preferentially contribute to the deletion of FV-reactive conventional T cells rather than the induction of nTregs carrying FV-reactive TCRs.

In summary, the loss of antigen-specific RTE production induced by thymic infection is a unique and powerful evasion strategy from antiviral $CD8^+$ T cell responses, especially when the functions of virus-specific $CD8^+$ T cells in the periphery are concomitantly severely compromised during the chronic phase of infection. Similar synergistic negative consequences could be induced in chronic infection with other thymotropic viruses such as HIV, although mechanisms of thymic failure may differ. In fact, HIV is known to cause thymotoxic infection that prevents adequate T cell generation [50], while FV infection does not affect thymocyte differentiation in general. There is no doubt that reinvigoration of exhausted virus-specific $CD8^+$ T cells in the periphery is a primary therapeutic target as we have shown in the case of acute FV infection [21]. However, as successful recovery from AIDS under anti-retroviral therapy is largely owing to the thymus-driven immune reconstitution, careful monitoring of the thymic function would be required in cases of thymotropic virus infection.

Materials and Methods

Ethics statements

The studies utilizing laboratory animals were carried out in strict accordance with the Act on Welfare and Management of Animals of the Government of Japan and the Regulations for the Care and Use of Laboratory Animals of Kinki University. The protocol for the present study was approved by the Institutional Animal Experimentation Committee of Kinki University Faculty of Medicine (Permit Number: KAME-20-066). All surgery was performed under sodium pentobarbital anesthesia, and all efforts were made to minimize suffering.

Viruses, mice, cells and infection/injection

An original stock of B-tropic FV complex without contamination of lactate dehydrogenase-elevating virus was kindly provided by Kim Hasenkrug (NIH, NIAID, Rocky Mountain Laboratories, Hamilton, MT). FV was expanded, stored, and titered as previously described [51]. An infectious molecular clone of F-MuLV, FB29, was prepared from culture supernatant of chronically infected *Mus dunni* cells as previously described [51]. A plasmid harboring the permutated FB29 cDNA was kindly provided by Marc Sitbon (Institut de Génétique Moléculaire de Montpellier, Montpellier, France). To insert the OVA epitope (SIINFEKL) into the C-terminus of the F-MuLV envelope protein in-frame, a pair of PCR primers that hybridize with the 3′ region of the F-MuLV genome and harbor the OVA sequence were used along with the above plasmid as the template (Figure S4B). Infectious F-MuLV-OVA was produced by transfecting *Mus dunni* cells with the mutant plasmid. Influenza virus A/HK-×31 was provided by David L. Woodland (Keystone Symposia, Silverthorne, CO). FBL3 is an F-MuLV-induced leukemia of B6 origin that expresses FV-related antigens [21]. EL-4 (a T cell lymphoma line derived from B6 mice) and E.G7 (EL-4 cells expressing OVA protein) were purchased from ATCC (Manassas, VA). C57BL/6NCrSlc (B6) mice were purchased from Japan SLC, Inc. (Shizuoka, Japan). A/WySnJ, B6.PL-*Thy1*^{a}/CyJ (Thy1.1; $CD90.1^+$) and B6.SJL-*Ptprc*^{a}*Pepc*^{b}/BoyJ (Pep/Boy; $CD45.1^+$) mice were purchased from The Jackson Laboratory (Bar Harbor, ME). OT-1 TCR transgenic mice with the B6 background (OT-1 mice) were kindly provided by Miyuki Azuma (Tokyo Medical and Dental University, Tokyo, Japan) with the permission of William R. Heath (University of Melbourne, Victoria Australia) [52]. OT-1 and Thy1.1 mice were crossed and F_2 progeny mice were selected for OT-1 TCR and Thy1.1 homozygosity by using monoclonal antibody (mAb) specific for mouse TCR Vα2, CD90.1 and CD90.2. OT-1-Thy1.1 mice thus

obtained were >98% Vα2$^+$ among CD8$^+$ T cells, CD90.1$^+$ and CD90.2$^-$. (OT-1-Thy1.1× A/WySnJ)F$_1$ mice were confirmed to be OT-1 TCR$^+$ and Thy1.1$^+$ and used in this study, and T cells separated from the above F$_1$ mice are termed OT-1 T cells in the text. *Rag1*-GFP knock-in mice with the B6 background have been described [53]. Animals were housed and bred in the Experimental Animal Facilities at Kinki University Faculty of Medicine under specific pathogen-free conditions. Due to a mutation in the intron of the *Stk* gene, B6 mice lack the expression of sf-Stk, and are resistant to SFFV-induced expansion of virus-infected erythroblasts and resultant splenomegaly [11,12]. As this erythroid cell expansion induced during the early phase of infection has been shown to be the major cause of severe exhaustion of virus-specific CD8$^+$ T cells [21], we used B6AF$_1$ mice that express sf-Stk in this study. Both male and female B6AF$_1$ mice, 6 to 10 weeks old, were infected intravenously (i.v.) either with 1,000 spleen focus-forming units (SFFU) of FV or with 2,000 focus-forming units of F-MuLV-OVA plus 1,000 SFFU of FV (termed FV-OVA). For tumor rejection experiments, mice were injected subcutaneously (s.c.) with 5×10^6 of FBL3 or EL-4 cells. Some experimental mice were challenged intranasally (i.n.) with 300 egg infective dose 50 (EID$_{50}$) of ×31.

Tissue harvest and flow cytometry

Mice were sacrificed at the indicated time points and single-cell suspensions from each tissue were obtained by straining through nylon mesh, depleted of erythrocytes in buffered ammonium chloride, and panned on goat anti-mouse IgG (H+L) (KPL, Gaithersburg, MD) for tetramer staining [21]. Live-cell counts were determined by trypan blue exclusion. Isolated cells were incubated with anti-CD16/32 (BD Biosciences, San Diego, CA) for 15 min on ice to prevent test antibodies (Abs) from binding to Fc receptors, and then stained either with APC-conjugated F-MuLV gag$_{75-83}$/D^b tetramer, influenza virus nucleoprotein (NP)$_{366-374}$/D^b tetramer, or OVA$_{257-264}$/K^b tetramer for 1 h at room temperature. All tetramers were generated at the Trudeau Institute Molecular Biology Core (Saranac Lake, NY). Tetramer-labeled cells were then washed and stained with FITC-, PE-, PerCP/Cy5.5-, or APC-conjugated antibodies for 30 min on ice. Antibodies reactive to the following molecules were purchased from BioLegend (San Diego, CA): CD3, CD4, CD8, CD11b, CD11c, CD19, CD44, CD69, CD80, CD90.1, CD90.2, PD-1, LAG-3, B220, Ly51, TCR Vα2, and EpCAM. Purified anti-F-MuLV envelope gp70 mAb, clone 720 [43], anti-F-MuLV gag p15 mAb, clone 34 [54], or mouse IgG$_1$ isotype control, clone 1B7, were labeled with biotin by using NHS-PEG$_4$-Biotin (Thermo Scientific, Waltham, MA) or with FITC by using Fluorescein Labeling Kit-NH$_2$ (Dojindo Molecular Technologies, Inc., Rockville, MD) as described [55]. Labeled streptavidin was purchased from BioLegend. Samples were run on a FACSCalibur or a FACSAria (BD Biosciences). All data were analyzed with FlowJo software (Tree Star, Ashland, OR).

In vitro restimulation and intracellular cytokine staining

Splenocytes isolated from infected mice as described above were seeded in 96-well plates at a concentration of 1×10^6 cells per well. Cells were incubated in the presence of Alexa488-conjugated anti-CD107a (BioLegend), monensin A (BioLegend) and either F-MuLV gag$_{75-83}$ peptide (5 μM), influenza NP$_{366-374}$ peptide (5 μM), OVA$_{257-264}$ peptide (5 μM), or anti-CD3 (4 μg/ml) (eBiosciences, San Diego, CA) for 2 h at 37°C; brefeldin A (50 μg/ml) was then added, and the incubation was continued for an additional 4 h. Surface staining for CD8 was performed as described above, and the cells were fixed and permeabilized with the Cytofix Cytoperm kit (BD Bioscience). For the detection of intracellular IFN-γ and IL-2, the cells were incubated for 15 min in the Perm/Wash buffer followed by incubation in the same buffer with anti-IFN-γ (BioLegend) and anti-IL-2 (BD Bioscience) for 1 h; the cells were then washed and analyzed as described above. To correct for background variations between experiments, we subtracted the percentage of IFN-γ$^+$, IL-2$^+$ or CD107a$^+$ cells among CD8$^+$ T cells without stimulation from the percentage of IFN-γ$^+$, IL-2$^+$ or CD107a$^+$ cells following peptide stimulation, for each individual mouse.

Infectious center assays

Cells prepared from each tissue were serially diluted and plated in duplicate at concentrations between 1×10^2 and 1×10^6 cells onto monolayers of *Mus dunni* cells. After being washed and fixed with methanol on the second day of coculturing, cells were stained with biotinylated mAb 720, and F-MuLV-infected foci were visualized by using Elite ABC Kit (Vector Laboratories, Burlingame, CA) as described [21].

Immunohistochemistry

The thymuses from naïve or FV-infected animals were harvested, embedded in OCT compound (Sakura Finetek, Tokyo Japan), and frozen in liquid nitrogen. Frozen sections (6 μm) were fixed with 4% paraformaldehyde for 10 min. After quenching endogenous biotin activity, sections were stained with combinations of PE-conjugated anti-CD11c, anti-ER-TR4 (specific for cortical thymic epithelial cells; cTECs), anti-ER-TR5 (specific for medullary thymic epithelial cells; mTECs) [56], biotin-conjugated anti-F-MuLV gag p15, clone 690 [57], and biotin-conjugated anti-F-MuLV gag p30, clone R18-7 [54]. Secondary antibodies, PE-conjugated anti-rat IgM, PE-conjugated anti-rat IgG, and AF488-conjugated streptavidin were used to visualize cTEC, mTEC and FV antigens, respectively. All frozen sections were observed and images recorded with a fluorescence microscope (BioZero; Keyence Japan).

Thymectomy and thymus transplantation

Day 5 neonatal pups were thymectomized. Five weeks later, mice were injected with purified anti-CD8 (2.43) and anti-CD4 (GK1.5) antibodies to deplete T cells in the periphery. A thymic lobe from FV-infected (2–3 weeks post infection) or age-matched uninfected donors was grafted under the kidney capsule. Six weeks later, mice were challenged with either FBL3 or infected with ×31.

Fetal thymus organ culture (FTOC)

Thymic stromal cells of B6AF$_1$ mice were prepared from E15.5 fetal thymus lobes that were cultured for 5 days in the presence of 2-deoxyguanosine [22]. OT-1 DP thymocytes were sorted from adult (OT-1-Thy1.1× A/WySnJ)F$_1$ mice. Thymocytes, thymic DCs or TECs from B6AF$_1$ mice infected with FV-OVA 21 days prior to the preparation were sorted as third populations. CD45-negative cells were enriched by depleting CD90$^+$ cells with a magnetic cell sorter (BD Bioscience) prior to sorting of thymic DC and TEC populations. Thymic stromal cells ($2–3\times10^5$) and OT-1 DP thymocytes ($3–5\times10^5$) were reaggregated and organ-cultured for 4 days in the presence of each third population ($0.5–2\times10^5$) as described [22].

OT-1 cell transfer

Splenocytes from (OT-1-Thy1.1× A/WySnJ)F$_1$ mice were enriched for CD8$^+$ cells by negative selection using Ab-conjugated

micromagnetic beads as described [58]. Cells were then stained with anti-CD44-FITC, and $CD44^{lo}$ cells were sorted using FACSVantage cell sorter with DIVA enhancement software (BD Bioscience). A total of $1–2\times10^7$ cells were transferred into recipient $B6AF_1$ mice infected with either FV or FV-OVA 42 days prior to the cell transfer.

Real-Time PCR

Total RNA was purified from the spleen, BM, and thymus of FV-infected mice using RNeasy Blood & Tissue kit (Qiagen, Hilden, Germany) and cDNA synthesis was performed by using PrimeScript RT reagent Kit (Takara Bio Inc., Shiga, Japan). The viral DNA fragments were amplified from 0.5 μg or 1 μg of total cDNA and were quantified using Platinum Quantitative PCR SuperMix-UDG with ROX (Life Technologies, Carlsbad, CA) and a Prism 7900HT Real-Time PCR system (Life Technologies). PCR primers and TaqMan probes for the differential detection of F-MuLV and SFFV cDNAs were designed on the *env* portion of each provirus: primers 5′-AAGTCTCCCCCCGCCTCTA-3′ and 5′-AGTGCCTGGTAAGCTCCCTGT-3′, and a FAM-labeled probe 5′-ACTCCCACATTGATTTCCCCGTCC-3′ for the detection of F-MuLV, and primers 5′-TCTAACCTCAC-CAACCCTGAT-3′ and 5′-TTTTAGGGCAATGGTATGAT-TAAAATAA-3′, and a FAM-labeled probe 5′-CCTAGTGT-CTGGACCCCCCTATTACGAGG-3′ for the detection of SFFV [59]. After initial incubations at 50°C for 2 min and 95°C for 10 min, 40 cycles of amplification were carried out at 95°C for 30 sec and at 58°C for 1 min. A TaqMan rodent GAPDH control reagent (Life Technologies) was used as an internal control. Standard curves obtained by using plasmids containing the *env* gene of each virus as templates were linear over a range of $10–10^6$ copies in the above reaction.

Statistical analysis

Statistical analyses were performed using Prism software (GraphPad Software, Inc., San Diego, CA). Methods of comparison and corrections for multiple comparisons are indicated in each relevant figure legend.

Accession numbers

Friend murine leukemia virus FB29 complete genome (accession number: Z11128).

Supporting Information

Figure S1 Virus-specific $CD8^+$ T cells in mice chronically infected with FV are non-responsive to the viral antigen. (A) FV-infected (6–8 weeks post infection) and age-matched uninfected mice were injected s.c. with FBL3 tumor cells (5×10^6). (B) At day 42–56 after infection (Before tumor injection) cells purified from the BM (upper panels) and spleen (lower panels) were stained with the indicated Abs and F-MuLV $gag_{75–83}/D^b$ tetramer. Shown are representative staining patterns for CD8 and the tetramer of $CD8^+$ T cells, and PD-1, CD69, LAG-3 and Tim-3 on $tetramer^+$ cells. (C) At day14 after FBL3 injection, splenocytes were isolated and stained with the indicated Abs and F-MuLV $gag_{75–83}/D^b$ tetramer. Shown are representative staining patterns for CD8 and the tetramer of $CD8^+$ T cells. (D) Fractions of spleen cells were stimulated with the $gag_{75–83}$ peptide or cultured without stimulation (Medium). The intracellular expression of IFN-γ and the surface expression of CD107a were measured by flow cytometry. Shown are representative staining patterns for intracellular IFN-γ and surface CD107a expression of stimulated and unstimulated $CD8^+$ T cells. Tumor sizes (E) and host survival (F) are shown for uninfected (upper panels) and FV-infected (lower panels) animals ($n=6–11$). Note that lines with tumor size zero in panel E include multiple individuals. Survival curves were compared between the uninfected and FV-infected groups by Mantel-Cox log-rank test: *, $p=0.0001$.
(DOC)

Figure S2 Viral antigen expression in each cell population in the thymus after FV or F-MuLV infection. $B6AF_1$ or B6 mice were infected with various doses of FV or F-MuLV. At day 14 after infection, cells in the thymus were isolated and stained with the indicated Abs. Shown are representative staining patterns and gating protocols of thymocytes. Data are representative of two independent experiments with essentially similar results.
(DOC)

Figure S3 Immunohistochemistry of the thymuses from FV-infected mice. Experiments were performed as described for Figure 3C. Arrowheads indicate cells doubly positive for the indicated cell surface marker and the viral antigen. Representative view-fields from those shown here are presented in Figure 3C.
(DOC)

Figure S4 Spleen weights and gp70 expression on B cells and erythroblasts after thymic transplantation. Experiments were performed as described for Figure 5. (A) Spleen weights were measured at day 14 after transplantation. (B) At day 14 after transplantation, splenocytes were isolated and stained with the indicated antibodies. Shown are representative staining patterns for gp70 on $CD19^+$ and $Ter119^+$ cells.
(DOC)

Figure S5 Construction of F-MuLV-OVA. (A) Schematic representation of the F-MuLV-OVA construct. A synthetic oligonucleotide encoding the SIINFEKL epitope was inserted in-frame at the 3′ end of the *env* gene (B) Detailed strategy for the generation of F-MuLV-OVA. Oligonucleotide primers harboring the OVA epitope sequence and hybridizing with the F-MuLV genome at the end of the *env* gene were used for PCR-based mutagenesis with the permutated molecular clone of F-MuLV as the template. F-MuLV genome sequence and base numbers shown are according to the database information (Z11128). The vertical arrow indicates the site of cleavage that generates fusogenic TM protein and R peptide [60]. (C) Splenocytes from naïve $B6AF_1$ mice were infected in vitro with either F-MuLV or F-MuLV-OVA. Cells were then cocultured with $CD8^+$ T cells purified from (OT-1-Thy1.1× A/WySnJ)F_1 mice (OT-1 cell). Shown are representative histograms for CD69 expression on OT-1 cells.
(DOC)

Figure S6 FACS profiles of cells from FTOC. Experiments were performed as described for Figure 6. Either tumor cells (A) or thymic cell populations purified from FV-OVA-infected mice (B) were used as the third population. Shown are representative dot plots of positive control settings (A) and experimental settings (B).
(DOC)

Figure S7 Post-thymic maturation of $CD8^+$ RTEs in mice chronically infected with FV. (*Rag1*-GFP×A.WySnJ)F_1 mice were infected with 1,000 SFFU of FV. Splenocytes were isolated at the indicated time-points and stained with the indicated Abs. Shown are dot plots for GFP expression among $CD4^+$ and $CD8^+$ T cells at day 42 after infection (A), and actual numbers of GFP^+CD8^+ T cells in either FV-infected or age-matched naïve

animals (B). No significant difference was observed between the groups. (C–D) Shown are representative staining patterns for PD-1, CD69 and CD44 of GFP^+CD8^+ T cells or GFP^-CD8^+ T cells (C), and for CD24, Qa2 and CD127 of GFP^-, GFP^{lo} or GFP^{hi} cells (D). (E–F) Splenocytes were stimulated *in vitro* with anti-CD3 Ab. The intracellular expression of IFN-γ and IL-2 were then measured by flow cytometry. Shown are representative staining patterns for IFN-γ and CD107a of GFP^+CD8^+ T cells (E), and frequencies of IFN-γ^+ cells and IL-2^+ cells among GFP^+CD8^+ T cells (F). Each symbol represents an individual mouse. Average percentages were compared between uninfected and FV-infected groups by two-way ANOVA with Bonferroni's corrections for multiple comparisons, and no significant difference was detected. Data are representative of two independent experiments with essentially equivalent results.
(DOC)

Acknowledgments

We thank Drs. Takeshi Nitta, Yoshiyuki Hakata, Jun Li, and Chihiro Motozono for helpful discussions and comments, Center for Instrumental Analysis, Central Research Facilities, Kinki University Faculty of Medicine (CRF) for assistance in flow cytometry, Center for Animal Experiments, CRF for help in thymectomy, Center for Morphological Analysis, CRF for help in histology, Drs. Miyuki Azuma and William R. Heath for providing OT-1 transgenic mice, Dr. David L. Woodland for providing influenza virus ×31, Drs. Michio Tomura, Takeshi Nitta and Yosuke Takahama for technical assistance with thymus transplantation and thymus organ culture and Mr. James Brian Dowell for critical reading and correction of the manuscript.

Author Contributions

Conceived and designed the experiments: ST. Performed the experiments: ST EK STK TM MF MK TC YK SK. Analyzed the data: ST MM. Contributed reagents/materials/analysis tools: ST EK MI NS MM. Wrote the paper: ST MM.

References

1. Kaech SM, Cui W (2012) Transcriptional control of effector and memory CD8(+) T cell differentiation. Nat Rev Immunol 12: 749–761.
2. Wherry EJ (2011) T cell exhaustion. Nat Immunol 12: 492–499.
3. Blackburn SD, Shin H, Haining WN, Zou T, Workman CJ, et al. (2009) Coregulation of CD8+ T cell exhaustion by multiple inhibitory receptors during chronic viral infection. Nat Immunol 10: 29–37.
4. Shin H, Blackburn SD, Blattman JN, Wherry EJ (2007) Viral antigen and extensive division maintain virus-specific CD8 T cells during chronic infection. J Exp Med 204: 941–949.
5. Vezys V, Masopust D, Kemball CC, Barber DL, O'Mara LA, et al. (2006) Continuous recruitment of naive T cells contributes to heterogeneity of antiviral CD8 T cells during persistent infection. J Exp Med 203: 2263–2269.
6. Wilson JJ, Pack CD, Lin E, Frost EL, Albrecht JA, et al. (2012) CD8 T cells recruited early in mouse polyomavirus infection undergo exhaustion. J Immunol 188: 4340–4348.
7. D'Souza WN, Hedrick SM (2006) Cutting edge: latecomer CD8 T cells are imprinted with a unique differentiation program. J Immunol 177: 777–781.
8. Miyazawa M, Tsuji-Kawahara S, Kanari Y (2008) Host genetic factors that control immune responses to retrovirus infections. Vaccine 26: 2981–2996.
9. Kim JW, Closs EI, Albritton LM, Cunningham JM (1991) Transport of cationic amino acids by the mouse ecotropic retrovirus receptor. Nature 352: 725–728.
10. Wang H, Kavanaugh MP, North RA, Kabat D (1991) Cell-surface receptor for ecotropic murine retroviruses is a basic amino-acid transporter. Nature 352: 729–731.
11. Li JP, D'Andrea AD, Lodish HF, Baltimore D (1990) Activation of cell growth by binding of Friend spleen focus-forming virus gp55 glycoprotein to the erythropoietin receptor. Nature 343: 762–764.
12. Persons DA, Paulson RF, Loyd MR, Herley MT, Bodner SM, et al. (1999) Fv2 encodes a truncated form of the Stk receptor tyrosine kinase. Nat Genet 23: 159–165.
13. Chesebro B, Bloom M, Wehrly K, Nishio J (1979) Persistence of infectious Friend virus in spleens of mice after spontaneous recovery from virus-induced erythroleukemia. J Virol 32: 832–837.
14. Dittmer U, He H, Messer RJ, Schimmer S, Olbrich AR, et al. (2004) Functional impairment of CD8(+) T cells by regulatory T cells during persistent retroviral infection. Immunity 20: 293–303.
15. Zelinskyy G, Dietze KK, Husecken YP, Schimmer S, Nair S, et al. (2009) The regulatory T-cell response during acute retroviral infection is locally defined and controls the magnitude and duration of the virus-specific cytotoxic T-cell response. Blood 114: 3199–3207.
16. Zelinskyy G, Kraft AR, Schimmer S, Arndt T, Dittmer U (2006) Kinetics of CD8+ effector T cell responses and induced CD4+ regulatory T cell responses during Friend retrovirus infection. Eur J Immunol 36: 2658–2670.
17. Robertson SJ, Messer RJ, Carmody AB, Hasenkrug KJ (2006) In vitro suppression of CD8+ T cell function by Friend virus-induced regulatory T cells. J Immunol 176: 3342–3349.
18. Myers L, Messer RJ, Carmody AB, Hasenkrug KJ (2009) Tissue-specific abundance of regulatory T cells correlates with CD8+ T cell dysfunction and chronic retrovirus loads. J Immunol 183: 1636–1643.
19. Iwashiro M, Messer RJ, Peterson KE, Stromnes IM, Sugie T, et al. (2001) Immunosuppression by CD4+ regulatory T cells induced by chronic retroviral infection. Proc Natl Acad Sci U S A 98: 9226–9230.
20. Dietze KK, Zelinskyy G, Gibbert K, Schimmer S, Francois S, et al. (2011) Transient depletion of regulatory T cells in transgenic mice reactivates virus-specific CD8+ T cells and reduces chronic retroviral set points. Proc Natl Acad Sci U S A 108: 2420–2425.
21. Takamura S, Tsuji-Kawahara S, Yagita H, Akiba H, Sakamoto M, et al. (2010) Premature terminal exhaustion of Friend virus-specific effector CD8+ T cells by rapid induction of multiple inhibitory receptors. J Immunol 184: 4696–4707.
22. Nitta T, Ohigashi I, Takahama Y (2013) The development of T lymphocytes in fetal thymus organ culture. Methods Mol Biol 946: 85–102.
23. Boursalian TE, Golob J, Soper DM, Cooper CJ, Fink PJ (2004) Continued maturation of thymic emigrants in the periphery. Nat Immunol 5: 418–425.
24. Makaroff LE, Hendricks DW, Niec RE, Fink PJ (2009) Postthymic maturation influences the CD8 T cell response to antigen. Proc Natl Acad Sci U S A 106: 4799–4804.
25. Wherry EJ, Blattman JN, Murali-Krishna K, van der Most R, Ahmed R (2003) Viral persistence alters CD8 T-cell immunodominance and tissue distribution and results in distinct stages of functional impairment. J Virol 77: 4911–4927.
26. Srinivasan M, Frauwirth KA (2009) Peripheral tolerance in CD8+ T cells. Cytokine 46: 147–159.
27. Young GR, Ploquin MJ, Eksmond U, Wadwa M, Stoye JP, et al. (2012) Negative selection by an endogenous retrovirus promotes a higher-avidity CD4+ T cell response to retroviral infection. PLoS Pathog 8: e1002709.
28. Gaulton GN (1998) Viral pathogenesis and immunity within the thymus. Immunol Res 17: 75–82.
29. Collavo D, Zanovello P, Biasi G, Chieco-Bianchi L (1981) T lymphocyte tolerance and early appearance of virus-induced cell surface antigens in Moloney-murine leukemia virus neonatally injected mice. J Immunol 126: 187–193.
30. Finke D, Acha-Orbea H (2001) Immune response to murine and feline retroviruses; Pantaleo G, Walker BD, editors. New Jersey: Humana Press, Inc. 125–157 p.
31. Zanovello P, Collavo D, Ronchese F, De Rossi A, Biasi G, et al. (1984) Virus-specific T cell response prevents lymphoma development in mice infected by intrathymic inoculation of Moloney leukaemia virus (M-MuLV). Immunology 51: 9–16.
32. Marshall DJ, Park BH, Korostoff JM, Gaulton GN (1995) Manipulation of the immune response by foreign gene expression in the thymus. Leukemia 9 Suppl 1: S128–132.
33. Jamieson BD, Somasundaram T, Ahmed R (1991) Abrogation of tolerance to a chronic viral infection. J Immunol 147: 3521–3529.
34. King CC, Jamieson BD, Reddy K, Bali N, Concepcion RJ, et al. (1992) Viral infection of the thymus. J Virol 66: 3155–3160.
35. Zajac AJ, Blattman JN, Murali-Krishna K, Sourdive DJ, Suresh M, et al. (1998) Viral immune evasion due to persistence of activated T cells without effector function. J Exp Med 188: 2205–2213.
36. Nobrega C, Roque S, Nunes-Alves C, Coelho A, Medeiros I, et al. (2010) Dissemination of mycobacteria to the thymus renders newly generated T cells tolerant to the invading pathogen. J Immunol 184: 351–358.
37. Nobrega C, Cardona PJ, Roque S, Pinto do OP, Appelberg R, et al. (2007) The thymus as a target for mycobacterial infections. Microbes Infect 9: 1521–1529.
38. Miller NE, Bonczyk JR, Nakayama Y, Suresh M (2005) Role of thymic output in regulating CD8 T-cell homeostasis during acute and chronic viral infection. J Virol 79: 9419–9429.
39. Edelmann SL, Marconi P, Brocker T (2011) Peripheral T cells re-enter the thymus and interfere with central tolerance induction. J Immunol 186: 5612–5619.
40. Hadeiba H, Lahl K, Edalati A, Oderup C, Habtezion A, et al. (2012) Plasmacytoid dendritic cells transport peripheral antigens to the thymus to promote central tolerance. Immunity 36: 438–450.
41. Bonasio R, Scimone ML, Schaerli P, Grabie N, Lichtman AH, et al. (2006) Clonal deletion of thymocytes by circulating dendritic cells homing to the thymus. Nat Immunol 7: 1092–1100.

42. Vogel AB, Haasbach E, Reiling SJ, Droebner K, Klingel K, et al. (2010) Highly pathogenic influenza virus infection of the thymus interferes with T lymphocyte development. J Immunol 185: 4824–4834.
43. Robertson MN, Miyazawa M, Mori S, Caughey B, Evans LH, et al. (1991) Production of monoclonal antibodies reactive with a denatured form of the Friend murine leukemia virus gp70 envelope protein: use in a focal infectivity assay, immunohistochemical studies, electron microscopy and western blotting. J Virol Methods 34: 255–271.
44. Lynch WP, Czub S, McAtee FJ, Hayes SF, Portis JL (1991) Murine retrovirus-induced spongiform encephalopathy: productive infection of microglia and cerebellar neurons in accelerated CNS disease. Neuron 7: 365–379.
45. Jordan MS, Boesteanu A, Reed AJ, Petrone AL, Holenbeck AE, et al. (2001) Thymic selection of CD4+CD25+ regulatory T cells induced by an agonist self-peptide. Nat Immunol 2: 301–306.
46. Maloy KJ, Powrie F (2001) Regulatory T cells in the control of immune pathology. Nat Immunol 2: 816–822.
47. Marodon G, Fisson S, Levacher B, Fabre M, Salomon BL, et al. (2006) Induction of antigen-specific tolerance by intrathymic injection of lentiviral vectors. Blood 108: 2972–2978.
48. Myers L, Joedicke JJ, Carmody AB, Messer RJ, Kassiotis G, et al. (2013) IL-2-independent and TNF-alpha-dependent expansion of Vbeta5+ natural regulatory T cells during retrovirus infection. J Immunol 190: 5485–5495.
49. Antunes I, Tolaini M, Kissenpfennig A, Iwashiro M, Kuribayashi K, et al. (2008) Retrovirus-specificity of regulatory T cells is neither present nor required in preventing retrovirus-induced bone marrow immune pathology. Immunity 29: 782–794.
50. Hazra R, Mackall C (2005) Thymic function in HIV infection. Curr HIV/AIDS Rep 2: 24–28.
51. Takeda E, Tsuji-Kawahara S, Sakamoto M, Langlois MA, Neuberger MS, et al. (2008) Mouse APOBEC3 restricts friend leukemia virus infection and pathogenesis in vivo. J Virol 82: 10998–11008.
52. Hogquist KA, Jameson SC, Heath WR, Howard JL, Bevan MJ, et al. (1994) T cell receptor antagonist peptides induce positive selection. Cell 76: 17–27.
53. Kuwata N, Igarashi H, Ohmura T, Aizawa S, Sakaguchi N (1999) Cutting edge: absence of expression of RAG1 in peritoneal B-1 cells detected by knocking into RAG1 locus with green fluorescent protein gene. J Immunol 163: 6355–6359.
54. Chesebro B, Britt W, Evans L, Wehrly K, Nishio J, et al. (1983) Characterization of monoclonal antibodies reactive with murine leukemia viruses: use in analysis of strains of friend MCF and Friend ecotropic murine leukemia virus. Virology 127: 134–148.
55. Tsuji-Kawahara S, Chikaishi T, Takeda E, Kato M, Kinoshita S, et al. (2010) Persistence of viremia and production of neutralizing antibodies differentially regulated by polymorphic APOBEC3 and BAFF-R loci in friend virus-infected mice. J Virol 84: 6082–6095.
56. Van Vliet E, Melis M, Van Ewijk W (1984) Monoclonal antibodies to stromal cell types of the mouse thymus. Eur J Immunol 14: 524–529.
57. McAtee FJ, Portis JL (1985) Monoclonal antibodies specific for wild mouse neurotropic retrovirus: detection of comparable levels of virus replication in mouse strains susceptible and resistant to paralytic disease. J Virol 56: 1018–1022.
58. Ogawa T, Tsuji-Kawahara S, Yuasa T, Kinoshita S, Chikaishi T, et al. (2011) Natural killer cells recognize friend retrovirus-infected erythroid progenitor cells through NKG2D-RAE-1 interactions In Vivo. J Virol 85: 5423–5435.
59. Tsuji-Kawahara S, Kawabata H, Matsukuma H, Kinoshita S, Chikaishi T, et al. (2013) Differential requirements of cellular and humoral immune responses for fv2-associated resistance to erythroleukemia and for regulation of retrovirus-induced myeloid leukemia development. J Virol 87: 13760–13774.
60. Yang C, Compans RW (1997) Analysis of the murine leukemia virus R peptide: delineation of the molecular determinants which are important for its fusion inhibition activity. J Virol 71: 8490–8496.

JVI Journals.ASM.org

Elimination of Friend Retrovirus in the Absence of CD8$^+$ T Cells

Sachiyo Tsuji-Kawahara, Masaaki Miyazawa

Department of Immunology, Kinki University Faculty of Medicine, Osaka-Sayama, Osaka, Japan

Friend retrovirus complex (FV) induces acute erythroid cell hyperplasia and massive splenomegaly followed by the emergence of fatal erythroleukemia upon inoculation into adult mice of susceptible strains (1–3). Because the disease can progress in the presence of host immune responses, FV has served as a useful model to study how retroviruses evade immune control (1, 3, 4). Depending on genotypes at several host loci, some strains of mice can eliminate virus-producing cells and recover from splenomegaly, while others progress rapidly to fatal pathology (1, 3, 5). Results from several research groups largely agree on the role of virus-neutralizing antibodies and CD4$^+$ T cells in immune control of FV infection (6–15). Natural killer cells also contribute to FV elimination and are essential for vaccine-induced protection of highly susceptible mice (8, 16). However, there are conflicting views on the role of CD8$^+$ T cells in FV control.

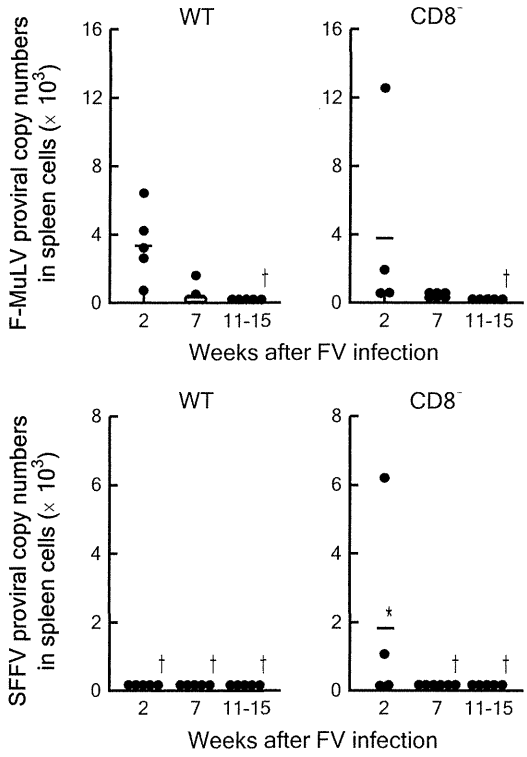

FIG 1 Changes in proviral copy numbers in the spleens of wild-type (WT) or CD8$^+$ T cell-deficient (CD8$^-$) B6 mice after inoculation of 5,000 spleen focus-forming units of FV. Wild-type B6 and CD8$^+$ T cell-deficient B6.129P2-β_2 m^{tm1Unc}/J mice carrying homozygous disruption of the β_2 microglobulin gene are those described in reference 24. Genomic DNA extraction and real-time PCR quantification of F-MuLV and SFFV proviruses were performed as described previously (24). Each closed circle represents an absolute copy number of F-MuLV or SFFV provirus in 100 ng of genomic DNA (equal to about 1.7 × 10^4 cells) detected from an individual mouse. Bars indicate averages for each genetic group and time point. *, significantly higher copy numbers than those in the WT animals [$P = 0.0159 < \alpha_3(0.05) = 0.0170$ by Mann-Whitney test for non-Gaussian distributions with Bonferroni's *post hoc* test for multiple comparisons]. †, undetectable in all animals examined.

Earlier studies associated major histocompatibility complex class I (MHC-I) alleles with spontaneous recovery from FV-induced splenomegaly, and FV-specific, CD8$^+$ cytotoxic T cells were detected (1, 5). Further, the recovery in *H2*^{b} mice was abrogated when CD8$^+$ T cells were depleted (6). On the other hand, by using FV-encoded epitopes recognized by CD4$^+$ T cells as peptide vaccines, we have shown that highly susceptible (BALB/c × C57BL/6)F$_1$ mice can still be protected from FV challenge and eliminate virus-producing cells in the absence of CD8$^+$ T cells (9). Interestingly, MHC-I genotypes influenced cytokine production from CD4$^+$ T cells upon FV infection (17, 18), indicating the possible indirect role of CD8$^+$ T cells.

C57BL/6 (B6) mice lack the expression of a short form of hematopoietic cell-specific receptor tyrosine kinase, Stk, and do not develop FV-induced erythroid cell proliferation (19). Some reports have indicated that CD8$^+$ T cells are essential in controlling FV infection in B6 mice, as infectious centers at an early time point after FV infection increased upon depletion of CD8$^+$ T cells (20–22). However, infectious centers were detected in the above-described reports with monoclonal antibody 720 (23) that reacts only with the helper component of FV, Friend murine leukemia virus (F-MuLV), but not with the pathogenic component, the spleen focus-forming virus (SFFV). In our recent work (24), SFFV was eliminated from B6 mice by 2 weeks after infection, and CD8$^+$ T cell-deficient B6 mice remained resistant to FV-induced disease development. Thus, the increase of F-MuLV infectious centers after CD8$^+$ T cell depletion, albeit statistically significant, may not reflect pathologically significant changes in SFFV load.

Here, we examined changes in SFFV copy numbers in CD8$^+$ T cell-deficient B6 mice after FV infection. CD8$^+$ T cell-deficient B6 mice nevertheless eliminated both F-MuLV and SFFV proviruses, though more slowly than the wild-type B6 mice did, as shown in Fig. 1. Thus, while CD8$^+$ T cells do contribute to control FV infection, they are not essential for the elimination of FV in B6 mice.

REFERENCES

1. **Chesebro B, Miyazawa M, Britt WJ.** 1990. Host genetic control of spontaneous and induced immunity to Friend murine retrovirus infection. Annu. Rev. Immunol. 8:477–499. http://dx.doi.org/10.1146/annurev.iy.08.040190.002401.
2. **Kabat D.** 1989. Molecular biology of Friend viral erythroleukemia. Curr.

Published ahead of print 13 November 2013

Address correspondence to masaaki@med.kindai.ac.jp.

doi:10.1128/JVI.03271-13

Top. Microbiol. Immunol. **148**:1–42. http://dx.doi.org/10.1007/978-3-642-74700-7_1.

3. **Miyazawa M, Tsuji-Kawahara S, Kanari Y.** 2008. Host genetic factors that control immune responses to retrovirus infections. Vaccine **26**:2981–2996. http://dx.doi.org/10.1016/j.vaccine.2008.01.004.
4. **Hasenkrug KJ, Dittmer U.** 2007. Immune control and prevention of chronic Friend retrovirus infection. Front. Biosci. **12**:1544–1551. http://dx.doi.org/10.2741/2167.
5. **Miyazawa M, Nishio J, Wehrly K, Chesebro B.** 1992. Influence of MHC genes on spontaneous recovery from Friend retrovirus-induced leukemia. J. Immunol. **148**:644–647.
6. **Robertson MN, Spangrude GJ, Hasenkrug K, Perry L, Nishio J, Wehrly K, Chesebro B.** 1992. Role and specificity of T-cell subsets in spontaneous recovery from Friend virus-induced leukemia in mice. J. Virol. **66**:3271–3277.
7. **Miyazawa M, Fujisawa R, Ishihara C, Takei YA, Shimizu T, Uenishi H, Yamagishi H, Kuribayashi K.** 1995. Immunization with a single T helper cell epitope abrogates Friend virus-induced early erythroid proliferation and prevents late leukemia development. J. Immunol. **155**:748–758.
8. **Iwanami N, Niwa A, Yasutomi Y, Tabata N, Miyazawa M.** 2001. Role of natural killer cells in resistance against Friend retrovirus-induced leukemia. J. Virol. **75**:3152–3163. http://dx.doi.org/10.1128/JVI.75.7.3152-3163.2001.
9. **Kawabata H, Niwa A, Tsuji-Kawahara S, Uenishi H, Iwanami N, Matsukuma H, Abe H, Tabata N, Matsumura H, Miyazawa M.** 2006. Peptide-induced immune protection of $CD8^+$ T cell-deficient mice against Friend retrovirus-induced disease. Int. Immunol. **18**:183–198. http://dx.doi.org/10.1093/intimm/dxh361.
10. **Nair SR, Zelinskyy G, Schimmer S, Gerlach N, Kassiotis G, Dittmer U.** 2010. Mechanisms of control of acute Friend virus infection by $CD4^+$ T helper cells and their functional impairment by regulatory T cells. J. Gen. Virol. **91**:440–451. http://dx.doi.org/10.1099/vir.0.015834-0.
11. **Pike R, Filby A, Ploquin MJ-Y, Eksmond U, Marques R, Antunes I, Hasenkrug K, Kassiotis G.** 2009. Race between retroviral spread and $CD4^+$ T-cell response determines the outcome of acute Friend virus infection. J. Virol. **83**:11211–11222. http://dx.doi.org/10.1128/JVI.01225-09.
12. **Messer RJ, Dittmer U, Peterson KE, Hasenkrug KJ.** 2004. Essential role for virus-neutralizing antibodies in sterilizing immunity against Friend retrovirus infection. Proc. Natl. Acad. Sci. U. S. A. **101**:12260–12265. http://dx.doi.org/10.1073/pnas.0404769101.
13. **Browne EP.** 2011. Toll-like receptor 7 controls the anti-retroviral germinal center response. PLoS Pathog. **7**:e1002293. http://dx.doi.org/10.1371/journal.ppat.1002293.
14. **Browne EP.** 2013. Toll-like receptor 7 inhibits early acute retroviral infection through rapid lymphocyte responses. J. Virol. **87**:7357–7366. http://dx.doi.org/10.1128/JVI.00788-13.
15. **Kane M, Case LK, Wang C, Yurkovetskiy L, Dikiy S, Golovkina T.** 2011. Innate immune sensing of retroviral infection via Toll-like receptor 7 occurs upon viral entry. Immunity **35**:135–145. http://dx.doi.org/10.1016/j.immuni.2011.05.011.
16. **Ogawa T, Tsuji-Kawahara S, Yuasa T, Kinoshita S, Chikaishi T, Takamura S, Matsumura H, Seya T, Saga T, Miyazawa M.** 2011. Natural killer cells recognize Friend retrovirus-infected erythroid progenitor cells through NKG2D-RAE-1 interactions *in vivo*. J. Virol. **85**:5423–5435. http://dx.doi.org/10.1128/JVI.02146-10.
17. **Peterson KE, Iwashiro M, Hasenkrug KJ, Chesebro B.** 2000. Major histocompatibility complex class I gene controls the generation of gamma interferon-producing $CD4^+$ and $CD8^+$ T cells important for recovery from Friend retrovirus-induced leukemia. J. Virol. **74**:5363–5367. http://dx.doi.org/10.1128/JVI.74.11.5363-5367.2000.
18. **Peterson KE, Stromnes I, Messer R, Hasenkrug K, Chesebro B.** 2002. Novel role of $CD8^+$ T cells and major histocompatibility complex class I genes in the generation of protective $CD4^+$ Th1 responses during retrovirus infection in mice. J. Virol. **76**:7942–7948. http://dx.doi.org/10.1128/JVI.76.16.7942-7948.2002.
19. **Persons DA, Paulson RF, Loyd MR, Herley MT, Bodner SM, Bernstein A, Correll PH, Ney PA.** 1999. *Fv2* encodes a truncated form of the Stk receptor tyrosine kinase. Nat. Genet. **23**:159–165. http://dx.doi.org/10.1038/13787.
20. **Zelinskyy G, Balkow S, Schimmer S, Schepers K, Simon MM, Dittmer U.** 2004. Independent roles of perforin, granzymes, and Fas in the control of Friend retrovirus infection. Virology **330**:365–374. http://dx.doi.org/10.1016/j.virol.2004.08.040.
21. **Zelinskyy G, Balkow S, Schimmer S, Werner T, Simon MM, Dittmer U.** 2007. The level of Friend retrovirus replication determines the cytolytic pathway of $CD8^+$ T-cell-mediated pathogen control. J. Virol. **81**:11881–11890. http://dx.doi.org/10.1128/JVI.01554-07.
22. **Manzke N, Akhmetzyanova I, Hasenkrug KJ, Trilling M, Zelinskyy G, Dittmer U.** 2013. $CD4^+$ T cells develop antiretroviral cytotoxic activity in the absence of regulatory T cells and $CD8^+$ T cells. J. Virol. **87**:6306–6313. http://dx.doi.org/10.1128/JVI.00432-13.
23. **Robertson MN, Miyazawa M, Mori S, Caughey B, Evans LH, Hayes SF, Chesebro B.** 1991. Production of monoclonal antibodies reactive with a denatured form of the Friend murine leukemia virus gp70 envelope protein: use in a focal infectivity assay, immunohistochemical studies, electron microscopy, and Western blotting. J. Virol. Methods **34**:255–271. http://dx.doi.org/10.1016/0166-0934(91)90105-9.
24. **Tsuji-Kawahara S, Kawabata H, Matsukuma H, Kinoshita S, Chikaishi T, Sakamoto M, Kawasaki Y, Miyazawa M.** 2013. Differential requirements of cellular and humoral immune responses for *Fv2*-associated resistance to erythroleukemia and for the regulation of retrovirus-induced myeloid leukemia development. J. Virol. **87**:13760–13774. http://dx.doi.org/10.1128/JVI.02506-13.

Virology 449 (2014) 82–87

Contents lists available at ScienceDirect

Virology

journal homepage: www.elsevier.com/locate/yviro

Defining HIV-1 Vif residues that interact with CBFβ by site-directed mutagenesis

Yusuke Matsui [a], Keisuke Shindo [a,*], Kayoko Nagata [a], Katsuhiro Io [a], Kohei Tada [a], Fumie Iwai [a], Masayuki Kobayashi [a], Norimitsu Kadowaki [a], Reuben S. Harris [b,c], Akifumi Takaori-Kondo [a]

[a] Department of Hematology and Oncology, Graduate School of Medicine, Kyoto University, Kyoto 606-8507, Japan
[b] Department of Biochemistry, Molecular Biology and Biophysics, University of Minnesota, MN 55455, United States
[c] Institute for Molecular Virology, University of Minnesota, MN 55455, United States

ARTICLE INFO

Article history:
Received 28 August 2013
Returned to author for revisions
13 September 2013
Accepted 1 November 2013
Available online 26 November 2013

Keywords:
HIV-1
Vif
CBFβ
Interaction
Host factors

ABSTRACT

Vif is essential for HIV-1 replication in T cells and macrophages. Vif recruits a host ubiquitin ligase complex to promote proteasomal degradation of the APOBEC3 restriction factors by poly-ubiquitination. The cellular transcription cofactor CBFβ is required for Vif function by stabilizing the Vif protein and promoting recruitment of a cellular Cullin5-RING ubiquitin ligase complex. Interaction between Vif and CBFβ is a promising therapeutic target, but little is known about the interfacial residues. We now demonstrate that Vif conserved residues E88/W89 are crucial for CBFβ binding. Substitution of E88/W89 to alanines impaired binding to CBFβ, degradation of APOBEC3, and virus infectivity in the presence of APOBEC3 in single-cycle infection. In spreading infection, NL4-3 with Vif E88A/W89A mutation replicated comparably to wild-type virus in permissive CEM-SS cells, but not in multiple APOBEC3 expressing non-permissive CEM cells. These results support a model in which HIV-1 Vif residues E88/W89 may participate in binding CBFβ.

Introduction

HIV-1 Vif is one of six viral accessory proteins and it is essential for the viral replication in T cells and macrophages (Gabuzda et al., 1992, 1994). Vif recruits host proteins, cullin 5 (CUL5), RING-box protein 2 (RBX2), elongin C (ELOC) and elongin B (ELOB), and forms a ubiquitin ligase complex that promotes poly-ubiquitination and proteasomal degradation of the APOBEC3 (A3) retrovirus restriction factors (Jäger et al., 2011; Marin et al., 2003; Sheehy et al., 2003; Shirakawa et al., 2006; Stopak et al., 2003; Yu et al., 2003). A3s are DNA cytosine deaminases that convert cytosines to uracils in single-stranded DNA (Chelico et al., 2006; Harris et al., 2003). In the absence of the Vif protein, at least two A3 family members, A3F and A3G, are efficiently incorporated into budding virions, where they deaminate cytosines in newly reverse-transcribed minus-strand virus DNA in target cells, leading to guanine to adenine hypermutation of the virus genome (Harris et al., 2003; Hultquist et al., 2011b; Sheehy et al., 2002; Zhang et al., 2003).

Amino acid sequences of HIV-1 Vif vary among viral strains, but more than ten regions of residues are conserved (Dang et al., 2010), and several conserved motifs have been shown to interact with host proteins. The BC-box motif ^{144}SLQYLA^{149} binds to ELOC (Mehle et al., 2004; Yu et al., 2004), and the HCCH motif ^{108}Hx$_5$Cx$_{17-18}$Cx$_{3-5}$H^{139} binds to CUL5 (Luo et al., 2005; Mehle et al., 2006). Furthermore, the N-terminal half of Vif contains distinct regions involved in the Vif-A3 protein-protein interactions; ^{11}WQxDRMR^{17} and ^{76}ExxW^{79} motifs are involved in neutralization of A3F (He et al., 2008; Russell and Pathak, 2007), whereas ^{40}YRHHY^{44} motif is involved in neutralization of A3G (Russell and Pathak, 2007); ^{22}KSLVK^{26} and ^{55}VxIPLx4-5Lxφx2YWxL^{72} motifs were reported to be involved in neutralization of both A3F and A3G (Chen et al., 2009; Dang et al., 2009; He et al., 2008; Pery et al., 2009), although there exists a report that K26 is required for neutralization of A3G, but not of A3F (Albin et al., 2010).

Recently, the transcription factor core binding factor-β (CBFβ) has been shown to be involved in the Vif ubiquitin ligase complex (Jäger et al., 2011; Zhang et al., 2011), and critical for its function by stabilizing the Vif protein in cells (Jäger et al., 2011), and enabling the recruitment of CUL5 (Zhang et al., 2011). There are two isoforms of CBFβ, and both isoforms stabilize Vif protein, enhance A3 degradation, and increase virion infectivity (Hultquist et al., 2011a). Thus, the interaction between Vif and CBFβ is a promising

* Correspondence to: Department of Hematology and Oncology, Graduate School of Medicine, 54 Shogoin-Kawaracho, Sakyo-ku, Kyoto, 606-8507 Japan. Tel: +81 75 751 4964. Fax: +81 75 751 4963.
E-mail address: shind009@kuhp.kyoto-u.ac.jp (K. Shindo).

0042-6822/$ - see front matter © 2013 Elsevier Inc. All rights reserved.
http://dx.doi.org/10.1016/j.virol.2013.11.004

therapeutic target, but little is known about the interfacial amino acids. Hultquist et al. reported that surface F68 residue of CBFβ is involved in binding and stabilizing Vif (Hultquist et al., 2012). Zhang et al. reported that W21 and W38 residues of Vif are required for binding to CBFβ by co-immunoprecipitation experiments (Zhang et al., 2011; Kim et al., 2013). Furthermore, Kim et al. recently suggested that L64 and I66 residues are involved in binding to CBFβ by co-purification in *Escherichia coli* (Kim et al., 2013).

Because a previous study indicated that a hydrophilic region ^{88}EWRKKR^{93} is essential for Vif expression and HIV-1 replication (Fujita et al., 2003), we hypothesized that conserved residues E88 and W89 in this region may be required for CBFβ binding. In this study, we generated amino acid substitution mutants of these residues as well as W21 and W38, and simultaneously analyzed both binding to CBFβ and Vif-mediated degradation of A3F and A3G. We show that the conserved residues E88 and W89 of HIV-1 Vif are directly involved in CBFβ binding and Vif-mediated degradation of A3F and A3G.

Results

The conserved residue W89 of HIV-1 Vif is required for the interaction with CBFβ

To test our hypothesis that conserved residues E88 and W89 may be required for CBFβ binding, we generated nine Vif amino acid substitution mutants, D14A/R15A, W21A, W38A, Y40A, Y69A, G84D, E88A, W89A, and E88A/W89A (Fig. 1A). W21 and W38 were reported to be involved in CBFβ binding (Zhang et al., 2011), D14 and R15 for APOBEC3F binding (Russell and Pathak, 2007), Y40 for A3G binding (Russell and Pathak, 2007), Y69 and G84 for both A3F and A3G binding (Dang et al., 2010; Pery et al., 2009). All of these residues are highly conserved, suggesting that they could be involved in CBFβ binding region of Vif. We first performed co-immunoprecipitation experiments in 293T cells by over-expression of Vif with C-terminal myc tag. Vif is a relatively unstable protein with a short half-life and it is degraded by the cellular proteasome (Dussart et al., 2004; Fujita et al., 2004; Mehle et al., 2004). Mouse double minute 2 homolog (MDM2) is the E3 ubiquitin ligase which targets Vif for degradation (Izumi et al., 2009). Because it has been reported that Vif degradation is accelerated in the absence of CBFβ, and that treatment with the proteasome inhibitor MG132 reverses this effect (Jäger et al., 2011), we used MG132 to minimize proteasomal proteolysis of Vif in cell culture and immunoprecipitation experiments. Although we transfected with the same amount of plasmid DNA, expression levels of E88A, W38A, D14/R15AA, Y40A, Y69A and G84D were comparable to wild-type Vif, but those of W89A, E88/W89A and W21A mutants were obviously impaired (Fig. S1, 2nd top panel). These modest expression levels of these mutants can be simply explained by misfolding, but an alternative explanation is due to loss of CBFβ binding. The amounts of immunoprecipitated Vif protein showed a smaller variation, compared to expression levels (Fig. S1, bottom panel). More importantly, endogenous CBFβ co-precipitated with wild-type Vif, D14A/R15A, Y40A, G84D, and E88A, but not with W21A, W89A, or E88A/W89A (Fig. S1, 3rd top panel). W38A and Y69A showed intermediate results (Fig. S1, lanes 7 and 10, 3rd top panel). To exclude the possibility that low expression of W21A, W89A and E88A/W89A mutants caused the low amount of co-immunoprecipitated CBFβ, we compensated by increasing the amount of transfected plasmid DNA, and performed an additional round of co-immunoprecipitation experiments. Although expression levels of W21A, W89A and E88A/W89A mutants were now higher than wild-type Vif, endogenous CBFβ did not co-precipitate with these mutants (Fig. 1B). We next examined whether CUL5 co-precipitated with Vif mutants by immunoblotting with some of the samples of Fig. 1B, because CBFβ binding has been reported to be required for Vif to interact with CUL5 (Zhang et al., 2011). Endogenous CUL5 appeared to co-precipitate with wild-type Vif, but not with W21A, W38A, W89A, or E88A/W89A (Fig. 1C, 2nd bottom panel). All

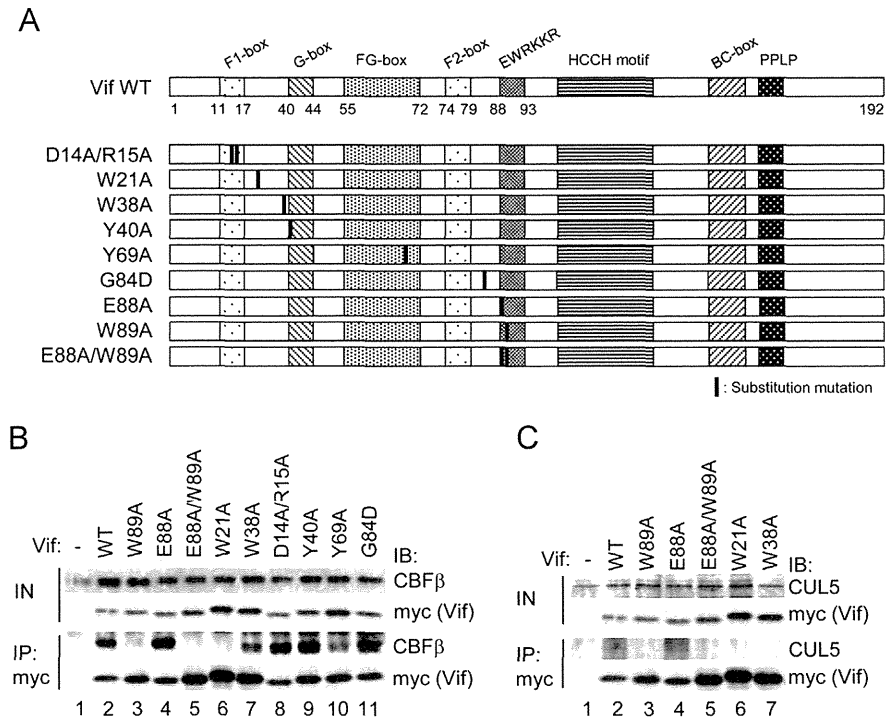

Fig. 1. Vif substitution mutants and binding capacity to CBFβ. (A) Schematic of Vif conserved motifs and nine substitution mutants generated. The residues substituted are indicated by bold lines. (B) Co-immunoprecipitation of endogenous CBFβ with Vif. Lysates of 293T cells transiently expressing myc-tagged Vif wild-type or mutant were immunoprecipitated by anti-myc serum. Samples were analyzed by immunoblotting with anti-CBFβ and anti-myc sera. (C) Co-immunoprecipitation of endogenous CUL5 with Vif. Samples from (B) were also analyzed with anti-CUL5 serum. Panels for Vif were re-produced from (B).

of these mutants of Vif bound to ELOB (Fig. S2), suggesting that they are not entirely misfolded proteins, although previous reports indicated that fragments of the Vif BC box is sufficient for binding to ELOB and ELOC (Bergeron et al., 2010; Wolfe et al., 2010). Altogether, these results suggest that W89 is involved in CBFβ binding, as well as W21 and W38.

The substitution of E88/W89 to alanines impairs Vif-mediated degradation of both A3F and A3G proteins

To examine whether the loss of binding to CBFβ causes impaired Vif-mediated degradation of A3 proteins, we next performed a series of co-transfection and immunoblot experiments. 293T cells were co-transfected with expression vectors for A3G with myc tag and Vif wild-type or mutant, and protein levels of A3G were analyzed by immunoblotting. To obtain comparable expression levels of each of the Vif mutants, we again adjusted the amount of plasmid DNA transfected. Co-transfection of wild-type Vif reduced APOBEC3G levels, but E88A/W89A, W21A or W38A did not (Fig. 2A, lanes 1, 2 and 7–12). E88A or W89A alone reduced A3G levels close to wild-type Vif (Fig. 2A, lanes 3–6). Because W21 and W38 are close to A3G binding residues of Vif, ^{40}YRHHY^{44}, the loss of A3G degradation by W21A or W38A might be caused by loss of A3G binding. To exclude this possibility, we next performed co-transfection experiments with Vif and A3F expression vectors and similar results were obtained (Fig. 2B). These results suggest that the substitution of E88/W89 as well as W21 and W38 to alanines leads to an impairment of Vif-mediated degradation of both A3F and A3G due to the loss of binding to CBFβ, not to A3F or A3G.

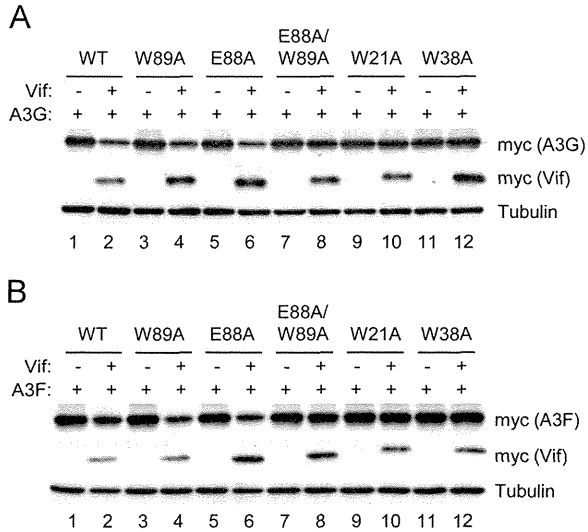

Fig. 2. Degradation of A3F and A3G by Vif. (A) Degradation of A3G. HEK293T cells were co-transfected with expression vectors for myc-tagged A3G and Vif wild-type or mutant, and protein levels of A3G and Vif were analyzed by immunoblotting with anti-myc serum and anti-tubulin antibody for loading control. The same amount of the A3G expression plasmid was transfected in each sample. (B) Degradation of A3F. Similar experiments to (A), but an A3F expression vector was used instead of that of A3G.

The substitution of E88/W89 to alanines impairs the ability of Vif to counteract the restriction by both A3F and A3G

To examine the ability of Vif mutants to counteract the restriction of HIV-1 by A3 proteins, we next performed single cycle infection experiments using luciferase-reporter viruses. The Vif mutations were introduced into pNL4-3 ΔEnv-Luc, and transfected into 293T cells with co-transfection of VSV-G expression plasmid in the presence or absence of co-transfection of A3G expression plasmid. Virus-containing supernatant was harvested and infectivity was measured by challenging to fresh 293T cells and assaying luciferase activity. Viruses with Vif mutations showed comparable infectivity in the absence of A3G, as expected (Fig. 3A). In the presence of A3G, virus with E88A mutation showed comparable infectivity to wild-type, but virus with W21A, W38A or E88A/W89A showed deeply impaired infectivity close to that of ΔVif (Fig. 3A). Virus with W89A showed intermediate and obviously impaired infectivity in the presence of A3G (Fig. 3A). We also performed these assays with A3F instead of A3G, and obtained similar results (Fig. 3B). These data indicate that E88/W89 residues as well as W21 and W38 are involved in Vif activity to counteract both A3F and A3G, suggesting these residues are involved in CBFβ binding, not A3F or A3G binding.

The substitution of E88/W89 to alanines impairs HIV-1 replication in non-permissive CEM cells

Finally, we performed spreading infection experiments in both permissive CEM-SS and multiple A3-expressing CEM cells. We introduced Vif mutations into NL4-3, a replication-competent

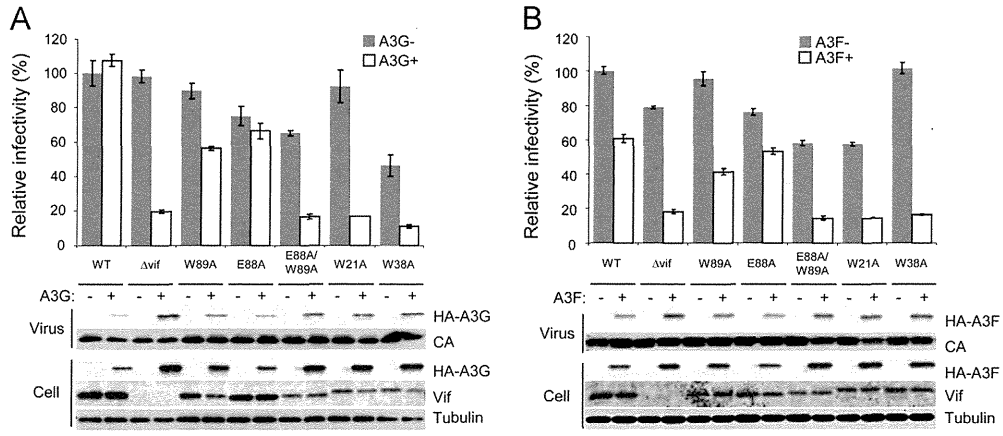

Fig. 3. Single-cycle infection experiments with VSV-G pseudo-typed viruses with vif mutations. (A) Counteracting abilities of Vif mutants against the restriction by A3G. 293T cells were transfected with pNL43/ΔEnv-Luc with vif mutation, together with pVSV-G, in the presence or absence of pcDNA3/HA-A3G. pNL43/ΔEnv-Luc without vif mutation and pNL43/ΔEnvΔvif-Luc were also used for control. Virus-containing supernatant was challenged to fresh 293T cells and infectivity was determined by luminometer. Values were normalized to that of the virus without vif mutation in the absence of A3G. Average and standard errors of 3 independent experiments are shown. Levels of A3G in cells and virions and Vif in cells were also analyzed by immunoblotting. (B) Counteracting abilities of Vif mutants against the restriction by A3F. Similar experiments to (A), but pcDNA3/HA-A3F was used instead of the A3G plasmid.

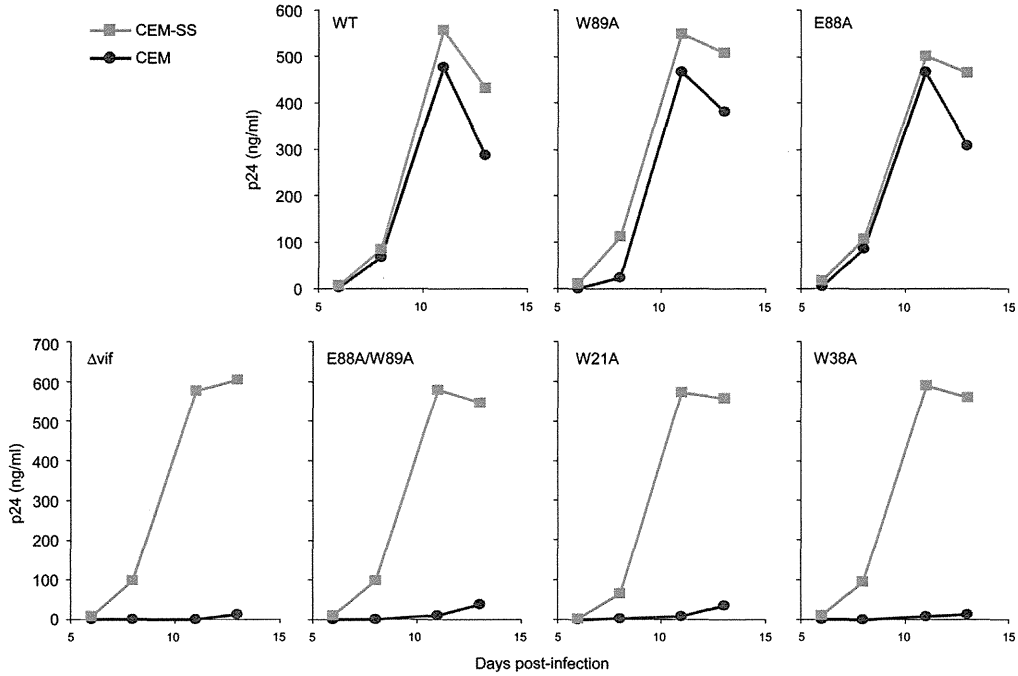

Fig. 4. Spreading infection of NL4-3 with vif mutations. The viruses were produced in 293T cells and challenged to permissive CEM-SS cells and nonpermissive CEM cells at MOI of 0.005. Culture supernatant was collected periodically and p24 levels were determined by ELISA.

molecular clone, and analyzed whether the substitution mutation impairs virus replication with spreading infection assays. Virus with E88A or W89A showed comparable replication profiles to wild-type virus in both CEM-SS and CEM cells. Virus with ΔVif, E88A/W89A, W21A, or W38A showed indistinguishable replication profiles to wild type in CEM-SS cells, as expected, whereas in CEM cells, showed deeply impaired replication profiles (Fig. 4). These results indicate that the residues E88/W89 as well as W21 and W38 are critical for Vif to counteract multiple A3s, suggesting that these residues are directly involved in CBFβ binding.

Discussion

In this study, we report that HIV-1 Vif residues E88 and W89 are involved in CBFβ binding, therefore in rendering Vif capable of stable expression and inducing ubiquitination of both A3F and A3G proteins. Fujita et al. reported that deletion or substitution of these residues impairs steady-state levels of Vif protein and virus replication in nonpermissive H9 cells and monocyte-derived macrophages (Fujita et al., 2003). We confirmed lower expression levels of substitution mutants using both Vif expression vectors and molecular clones of HIV-1. We also confirmed inefficient replication of virus with the mutation using another nonpermissive T cell line, CEM cells. These observations may be all explained by the loss of CBFβ binding.

Our results suggest that the single amino acid substitution mutant W89A does not bind to CBFβ, however this mutant is capable of degradation of A3F and A3G, and supporting replication of the virus in non-permissive CEM cells. This modest conflict may be due to the differences in experimental settings; co-immunoprecipitation experiments test the interactions *in vitro* in complex total cell lysates, and degradation experiments and infectivity experiments test Vif functionality in living cells.

Zhang et al. reported that Vif residues W21 and W38 are involved in binding to CBFβ, but functional correlation of these residues was not described (Zhang et al., 2011). We confirmed that these residues are critical for CBFβ binding, and further demonstrated that these residues are critical for degradation of both A3F and A3G, counteracting restriction by both A3F and A3G, and replication in nonpermissive, multiple A3-expressing cells.

Jäger et al. reported that CBFβ functions to up-regulate steady-state level of Vif protein by using cells with CBFβ knock-down (Jäger et al., 2011). We observed that the levels of Vif mutants that do not bind to CBFβ were obviously lower than that of wild-type Vif. Our observations confirmed and support the Jäger's report by the experiments with different settings.

Several E3 ligases including CUL5, NEDD4, and AIP4, have been reported to induce Vif ubiquitination, although biological implications have not been well defined (Dussart et al., 2004; Mehle et al., 2004). We previously reported that MDM2 targets for Vif as an E3 ligase to induce its ubiquitination and proteasomal degradation, and that the N-terminal region of Vif (residues 4–22) is required for MDM2 binding (Izumi et al., 2009). Because one of the CBFβ binding residues of Vif, W21, is located close to MDM2 binding region, the loss of CBFβ binding might facilitate ubiquitination and degradation of Vif by MDM2. Further investigations will be required to test this possibility.

We provide here the evidence indicating that residues W21, W38, E88 and W89 of HIV-1 Vif are involved in binding surface to CBFβ. Further studies on the Vif-CBFβ co-crystal structure will be the key to understanding Vif-CBFβ interaction surfaces, and to pharmaceutical applications of these pieces of information for patients with HIV-1 infection.

Materials and methods

Plasmid construction

C-terminally myc-tagged Vif expression plasmid, pDON-Vif-myc, was generated by amplifying NL4-3 vif coding sequence with primers ATA GGA TCC ATG GAA AAC AGA TG G CAG GTG GCA GGT GAT G and CGC GTC GAC CTA CAG ATC CTC TTC AGA GAT GAG TTT CTG CTC GTA GTG TCC ATT CAT TGT ATG GCT CCC, and inserting it into pDON-AI (Takara) at BamH I/Sal I sites. Expression plasmids for

Vif mutants were generated by a PCR-based method with properly mutated primers. HA-tagged expression plasmids for A3F and A3G were previously described (Shirakawa et al., 2006). N-terminally myc-tagged expression plasmids for A3F, pcDNA3-myc-A3F, was generated by amplifying coding sequences of human A3F with primers CTA GCT AGC ATG GAG CAG AAA CTC ATC TCT GAA GAG GAT CTG ATG AAG CCT CAC TTC AGA AAC ACA GTG G and GGG GTA CCT CAC TCG AGA ATC TCC TGC AGC TTG CTG, and inserting it into pcDNA3.1 (Invitrogen) at Nhe I/Kpn I sites. C-terminally myc-tagged expression plasmids for A3G, pcDNA3-A3G-myc, was generated by amplifying coding sequences of human A3G with primers ATA CTC GAG AAT GAA GCC TAC TTC AGA AAC ACA GTG and GGG GTA CCC TAC AGA TCC TCT TCA GAG ATG AGT TTC TGC TCG CAG TTT TCC TGA TTC TGG AGA ATG GC, and inserting it into pcDNA3.1 (Invitrogen) at Xho I/Kpn I sites. The luciferase-reporter HIV-1 plasmids for single-cycle infection, pNL43/ΔEnv-Luc and pNL43/ΔEnvΔvif-Luc were previously described (Shindo et al., 2003). Mutations in vif region of pNL43/ΔEnv-Luc and pNL4-3 were introduced by a PCR-based method using internal restriction sites, MSC I at position 4553, and EcoR I at position 5743.

Cell culture and transfection

293T cells were maintained in Dulbecco's modified Eagle's medium supplemented with 10% fetal bovine serum (FBS) and penicillin, streptomycin and glutamine (PSG). CEM and CEM-SS cells were maintained in RPMI1640 medium supplemented with 10% FBS and PSG. 293T cells on 6-well plates were transfected with about 1 μg of plasmid DNA in total using X-tremegene HP DNA transfection reagent (Roche) according to manufacturer's instruction.

Immunoblotting

Primary antibodies for immunoblotting against Vif, A3G and $p24^{Gag}$ were obtained from the NIH AIDS Research and Reference Reagent Program. Rabbit anti-CBFβ serum and mouse anti-Cul5 and anti-HA antibodies were purchased from Santa Cruz. Rabbit anti-myc serum was purchased from Sigma. Mouse anti-tubulin antibody was purchased from Covance. HRP-conjugated secondary antibodies against mouse and rabbit were purchased from GE Healthcare. We used a standard chemiluminescence protocol for immunoblotting with PVDF membrane (Millipore).

Immunoprecipitation

For co-immunoprecipitation to test interaction of Vif mutant to CBFβ, 293T cells were transfected with pDON-Vif-myc or its derivative mutant, treated with MG132 at concentration of 2.5 μM for 16 h, and lysed with co-IP buffer (25 mM HEPES, pH 7.4, 150 mM NaCl, 0.1% Triton X-100, 1 mM EDTA, 1mM $MgCl_2$) supplemented with protease inhibitor cocktail (Nacalai) and MG132. After centrifugation at 20,000 × *g* for 10 min, supernatant was mixed with 2 μg anti-myc rabbit serum (Sigma) for 1 h, and then mixed with 20 μl protein A sepharose (Pharmacia) for 1 h. Beads were washed with co-IP buffer 3 times, and bound protein was eluted with 1 x SDS sample buffer. Samples were analyzed by immunoblotting as described above.

Single-cycle infection

Luciferase encoding HIV-1 particles were produced by transiently transfecting 293T cells at 50% confluency using 0.8 μg pNL43/ΔEnv-Luc or derivative mutant, 0.2 μg pVSV-G and 0.02 μg pcDNA3/HA-A3F, pcDNA3/HA-A3G, or empty vector. After 48 h, virus-containing supernatants were harvested through PVDF filter with 0.45 μm pores (Millipore), and challenged to fresh 293T cells. After 48 h, cells were lysed with Passive lysis buffer (Promega) and luciferase activity was determined by luminometer (2030 Arvo X, Perkin Elmer) using Luciferase Assay System (Promega). Sample preparation of producer cells and virus for immunoblotting was performed as described (Haché et al., 2008).

Spreading infection

293T cells were transfected with NL4-3 molecular clone or derivative mutant, and virus-containing supernatant was harvested through PVDF filters with 0.45 μm pores (Millipore) after 2-day incubation. CEM-SS and CEM cells were inoculated with the supernatant at MOI of 0.005. The culture supernatants were harvested periodically, and analyzed for p24 by an HIV-1 p24 antigen ELISA kit (Zeptometrix).

Acknowledgments

We thank Dr. Y. Koyanagi for BL3 laboratory, Drs. J. Hultquist and A. Land in University of Minnesota for helpful discussion. The following materials were obtained through the AIDS Research and Reference Reagent Program, NIH: rabbit anti-Vif serum 2221 from Dr. Dana Gabuzda, anti-p24 Gag monoclonal antibody 6457 from Dr. Michael H. Malim, and rabbit anti-A3G serum 10201 from Dr. Jaisri Lingappa.

This study was partly supported by Grants-in-aid from the Ministry of Education, Culture, Sports, Science and Technology and from the Ministry of Health, Labor and Welfare in Japan. Work in the Harris lab was supported in part by grants from the National Institutes of Health (R01 AI064046 and P01 GM091743).

Appendix A. Supplementary material

Supplementary data associated with this article can be found in the online version at http://dx.doi.org/10.1016/j.virol.2013.11.004.

References

Albin, J.S., Haché, G., Hultquist, J.F., Brown, W.L., Harris, R.S., 2010. Long-term restriction by APOBEC3F selects human immunodeficiency virus type 1 variants with restored Vif function. J. Virol. 84 (19), 10209–10219.

Bergeron, J.R., Huthoff, H., Veselkov, D.A., Beavil, R.L., Simpson, P.J., Matthews, S.J., Malim, M.H., Sanderson, M.R., 2010. The SOCS-box of HIV-1 Vif interacts with ElonginBC by induced-folding to recruit its Cul5-containing ubiquitin ligase complex. PLoS Pathog 6 (6), e1000925.

Chelico, L., Pham, P., Calabrese, P., Goodman, M.F., 2006. APOBEC3G DNA deaminase acts processively 3′→5′ on single-stranded DNA. Nat. Struct. Mol. Biol. 13 (5), 392–399.

Chen, G., He, Z., Wang, T., Xu, R., Yu, X.F., 2009. A patch of positively charged amino acids surrounding the human immunodeficiency virus type 1 Vif SLVx4Yx9Y motif influences its interaction with APOBEC3G. J. Virol. 83 (17), 8674–8682.

Dang, Y., Davis, R.W., York, I.A., Zheng, Y.H., 2010. Identification of 81LGxGxxIxW89 and 171EDRW174 domains from human immunodeficiency virus type 1 Vif that regulate APOBEC3G and APOBEC3F neutralizing activity. J. Virol. 84 (11), 5741–5750.

Dang, Y., Wang, X., Zhou, T., York, I.A., Zheng, Y.H., 2009. Identification of a novel WxSLVK motif in the N terminus of human immunodeficiency virus and simian immunodeficiency virus Vif that is critical for APOBEC3G and APOBEC3F neutralization. J. Virol. 83 (17), 8544–8552.

Dussart, S., Courcoul, M., Bessou, G., Douaisi, M., Duverger, Y., Vigne, R., Decroly, E., 2004. The Vif protein of human immunodeficiency virus type 1 is posttranslationally modified by ubiquitin. Biochem. Biophys. Res. Commun. 315 (1), 66–72.

Fujita, M., Akari, H., Sakurai, A., Yoshida, A., Chiba, T., Tanaka, K., Strebel, K., Adachi, A., 2004. Expression of HIV-1 accessory protein Vif is controlled uniquely to be low and optimal by proteasome degradation. Microb. Infect. 6 (9), 791–798.

Fujita, M., Sakurai, A., Yoshida, A., Miyaura, M., Koyama, A.H., Sakai, K., Adachi, A., 2003. Amino acid residues 88 and 89 in the central hydrophilic region of human immunodeficiency virus type 1 Vif are critical for viral infectivity by enhancing the steady-state expression of Vif. J. Virol. 77 (2), 1626–1632.

Gabuzda, D.H., Lawrence, K., Langhoff, E., Terwilliger, E., Dorfman, T., Haseltine, W.A., Sodroski, J., 1992. Role of vif in replication of human immunodeficiency virus type 1 in CD4+ T lymphocytes. J. Virol. 66 (11), 6489–6495.

Gabuzda, D.H., Li, H., Lawrence, K., Vasir, B.S., Crawford, K., Langhoff, E., 1994. Essential role of vif in establishing productive HIV-1 infection in peripheral

blood T lymphocytes and monocyte/macrophages. J. Acquir. Immune Defic. Syndr. 7 (9), 908–915.
Haché, G., Shindo, K., Albin, J.S., Harris, R.S., 2008. Evolution of HIV-1 isolates that use a novel Vif-independent mechanism to resist restriction by human APOBEC3G. Curr. Biol. 18 (11), 819–824.
Harris, R.S., Bishop, K.N., Sheehy, A.M., Craig, H.M., Petersen-Mahrt, S.K., Watt, I.N., Neuberger, M.S., Malim, M.H., 2003. DNA deamination mediates innate immunity to retroviral infection. Cell 113 (6), 803–809.
He, Z., Zhang, W., Chen, G., Xu, R., Yu, X.F., 2008. Characterization of conserved motifs in HIV-1 Vif required for APOBEC3G and APOBEC3F interaction. J. Mol. Biol. 381 (4), 1000–1011.
Hultquist, J.F., Binka, M., LaRue, R.S., Simon, V., Harris, R.S., 2011a. Vif proteins of human and simian immunodeficiency viruses require cellular CBFbeta to degrade APOBEC3 restriction factors. J. Virol. 86 (5), 2874–2877.
Hultquist, J.F., Lengyel, J.A., Refsland, E.W., LaRue, R.S., Lackey, L., Brown, W.L., Harris, R.S., 2011b. Human and rhesus APOBEC3D, APOBEC3F, APOBEC3G, and APOBEC3H demonstrate a conserved capacity to restrict Vif-deficient HIV-1. J. Virol. 85 (21), 11220–11234.
Hultquist, J.F., McDougle, R.M., Anderson, B.D., Harris, R.S., 2012. HIV type 1 viral infectivity factor and the RUNX transcription factors interact with core binding factor beta on genetically distinct surfaces. AIDS Res. Hum. Retroviruses 28 (12), 1543–1551.
Izumi, T., Takaori-Kondo, A., Shirakawa, K., Higashitsuji, H., Itoh, K., Io, K., Matsui, M., Iwai, K., Kondoh, H., Sato, T., Tomonaga, M., Ikeda, S., Akari, H., Koyanagi, Y., Fujita, J., Uchiyama, T., 2009. MDM2 is a novel E3 ligase for HIV-1 Vif. Retrovirology 6, 1.
Jäger, S., Kim, D.Y., Hultquist, J.F., Shindo, K., LaRue, R.S., Kwon, E., Li, M., Anderson, B.D., Yen, L., Stanley, D., Mahon, C., Kane, J., Franks-Skiba, K., Cimermancic, P., Burlingame, A., Sali, A., Craik, C.S., Harris, R.S., Gross, J.D., Krogan, N.J., 2011. Vif hijacks CBF-beta to degrade APOBEC3G and promote HIV-1 infection. Nature 481 (7381), 371–375.
Kim, D.Y., Kwon, E., Hartley, P.D., Crosby, D.C., Mann, S., Krogan, N.J., Gross, J.D., 2013. CBFbeta stabilizes HIV Vif to counteract APOBEC3 at the expense of RUNX1 target gene expression. Mol. Cell 49 (4), 632–644.
Luo, K., Xiao, Z., Ehrlich, E., Yu, Y., Liu, B., Zheng, S., Yu, X.F., 2005. Primate lentiviral virion infectivity factors are substrate receptors that assemble with cullin 5-E3 ligase through a HCCH motif to suppress APOBEC3G. Proc. Nat. Acad. Sci. U.S.A. 102 (32), 11444–11449.
Marin, M., Rose, K.M., Kozak, S.L., Kabat, D., 2003. HIV-1 Vif protein binds the editing enzyme APOBEC3G and induces its degradation. Nat. Med. 9 (11), 1398–1403.
Mehle, A., Goncalves, J., Santa-Marta, M., McPike, M., Gabuzda, D., 2004. Phosphorylation of a novel SOCS-box regulates assembly of the HIV-1 Vif-Cul5 complex that promotes APOBEC3G degradation. Genes Dev. 18 (23), 2861–2866.
Mehle, A., Thomas, E.R., Rajendran, K.S., Gabuzda, D., 2006. A zinc-binding region in Vif binds Cul5 and determines cullin selection. J. Biol. Chem. 281 (25), 17259–17265.
Pery, E., Rajendran, K.S., Brazier, A.J., Gabuzda, D., 2009. Regulation of APOBEC3 proteins by a novel YXXL motif in human immunodeficiency virus type 1 Vif and simian immunodeficiency virus SIVagm Vif. J. Virol. 83 (5), 2374–2381.
Russell, R.A., Pathak, V.K., 2007. Identification of two distinct human immunodeficiency virus type 1 Vif determinants critical for interactions with human APOBEC3G and APOBEC3F. J. Virol. 81 (15), 8201–8210.
Sheehy, A.M., Gaddis, N.C., Choi, J.D., Malim, M.H., 2002. Isolation of a human gene that inhibits HIV-1 infection and is suppressed by the viral Vif protein. Nature 418 (6898), 646–650.
Sheehy, A.M., Gaddis, N.C., Malim, M.H., 2003. The antiretroviral enzyme APOBEC3G is degraded by the proteasome in response to HIV-1 Vif. Nat. Med. 9 (11), 1404–1407.
Shindo, K., Takaori-Kondo, A., Kobayashi, M., Abudu, A., Fukunaga, K., Uchiyama, T., 2003. The enzymatic activity of CEM15/Apobec-3G is essential for the regulation of the infectivity of HIV-1 virion but not a sole determinant of its antiviral activity. J. Biol. Chem. 278 (45), 44412–44416.
Shirakawa, K., Takaori-Kondo, A., Kobayashi, M., Tomonaga, M., Izumi, T., Fukunaga, K., Sasada, A., Abudu, A., Miyauchi, Y., Akari, H., Iwai, K., Uchiyama, T., 2006. Ubiquitination of APOBEC3 proteins by the Vif-Cullin5-ElonginB-ElonginC complex. Virology 344 (2), 263–266.
Stopak, K., de Noronha, C., Yonemoto, W., Greene, W.C., 2003. HIV-1 Vif blocks the antiviral activity of APOBEC3G by impairing both its translation and intracellular stability. Mol. Cell 12 (3), 591–601.
Wolfe, L.S., Stanley, B.J., Liu, C., Eliason, W.K., Xiong, Y., 2010. Dissection of the HIV Vif interaction with human E3 ubiquitin ligase. J Virol 84 (14), 7135–7139.
Yu, X., Yu, Y., Liu, B., Luo, K., Kong, W., Mao, P., Yu, X.F., 2003. Induction of APOBEC3G ubiquitination and degradation by an HIV-1 Vif-Cul5-SCF complex. Science 302 (5647), 1056–1060.
Yu, Y., Xiao, Z., Ehrlich, E.S., Yu, X., Yu, X.F., 2004. Selective assembly of HIV-1 Vif-Cul5-ElonginB-ElonginC E3 ubiquitin ligase complex through a novel SOCS box and upstream cysteines. Genes Dev. 18 (23), 2867–2872.
Zhang, H., Yang, B., Pomerantz, R.J., Zhang, C., Arunachalam, S.C., Gao, L., 2003. The cytidine deaminase CEM15 induces hypermutation in newly synthesized HIV-1 DNA. Nature 424 (6944), 94–98.
Zhang, W., Du, J., Evans, S.L., Yu, Y., Yu, X.F., 2011. T-cell differentiation factor CBF-beta regulates HIV-1 Vif-mediated evasion of host restriction. Nature 481 (7381), 376–379.

STEM CELLS®

TISSUE-SPECIFIC STEM CELLS

C/EBPβ Expressed by Bone Marrow Mesenchymal Stromal Cells Regulates Early B-cell Lymphopoiesis

Satoshi Yoshioka[1,2], Yasuo Miura[2,#], Hisayuki Yao[2], Sakiko Satake[2], Yoshihiro Hayashi[2,3], Akihiro Tamura[2], Terutoshi Hishita[4], Tatsuo Ichinohe[5], Hideyo Hirai[2], Akifumi Takaori-Kondo[1] and Taira Maekawa[2]

[1]Department of Hematology/Oncology, Graduate School of Medicine, Kyoto University and [2]Department of Transfusion Medicine & Cell Therapy, Kyoto University Hospital, Kyoto, 606-8507, Japan. [3]Division of Gastroenterology and Hematology, Shiga University of Medical Science, Shiga, 520-2192, Japan. [4]Department of Hematology, National Himeji Medical Center, Hyogo, 670-8520, Japan. [5] Department of Hematology and Oncology, Research Institute for Radiation Biology and Medicine, Hiroshima University, Hiroshima 734-8553, Japan.

Key Words. B lymphocytes • bone marrow • CCAAT/enhancer-binding protein β • mesenchymal stromal cells.

ABSTRACT

The transcription factor CCAAT/enhancer-binding protein β (C/EBPβ) regulates the differentiation of a variety of cell types. Here, the role of C/EBPβ expressed by bone marrow mesenchymal stromal cells (BMMSCs) in B-cell lymphopoiesis was examined. The size of the precursor B-cell population in bone marrow was reduced in C/EBPβ-knockout (KO) mice. When bone marrow cells from C/EBPβ-KO mice were transplanted into lethally irradiated wild-type (WT) mice, which provide a

Author contributions: S.Y.: conception and design, collection of data, data analysis and interpretation, and manuscript writing; Y.M.: conception and design, financial support, collection of data, data analysis and interpretation, and manuscript writing; H.Y.: conception and design, collection of data, data analysis and interpretation, and manuscript writing; S.S.: collection of data, and data analysis and interpretation; Y.H.: data analysis and interpretation; A.T.: data analysis and interpretation; T.H.: conception and design, collection of data, and data analysis and interpretation; T.I.: conception and design, financial support, data analysis and interpretation, and manuscript writing; H.H.: conception and design, financial support, collection of data, data analysis and interpretation, and manuscript writing; A.T.-K.: conception and design, data analysis and interpretation, and manuscript writing; T.M.: conception and design, financial support, data analysis and interpretation, and manuscript writing. All authors listed approve this manuscript.

[#]Correspondence: Yasuo Miura, M.D., Ph.D. , Address: Department of Transfusion Medicine & Cell Therapy, Kyoto University Hospital, 54 Kawaharacho, Shogoin, Sakyo-ku, Kyoto, 606-8507, Japan., Tel: +81-75-751-3630, Fax: +81-75-751-4283, E-mail: ym58f5@kuhp.kyoto-u.ac.jp;
Grants: This work was supported in part by a Grant-in-Aid from the Ministry of Education, Culture, Sports, Science and Technology in Japan (to Y.M., Y.H., T.I., H.H., and T.M), a Grant-in-Aid from the Japan Science and Technology Agency (to Y.M.), and a Grant-in-Aid from the Ministry of Health, Labour and Welfare in Japan (to T.I. and T. M). This work was also supported in part by the Japan Leukemia Research Fund (to Y.M), the Kyoto University Translational Research Center (to Y.M), the Ichiro Kanehara Foundation (to Y.M. and S.Y.), the National Cancer Center Research and Development Fund (to T.M., 23-A-23), the Kobayashi Foundation for Cancer Research (to T.M.), the Cell Science Research Foundation (to Y.M.), and the Senshin Medical Research Foundation (to T.M.).; Received January 21, 2013; accepted for publication September 05, 2013. 1066-5099/2013/$30.00/0 doi: 10.1002/stem.1555